



Calhoun: The NPS Institutional Archive
DSpace Repository

Theses and Dissertations

1. Thesis and Dissertation Collection, all items

1974

Formulation and comparison of instantaneous distortion indices for assessing compressor stall.

Vann, John Lloyd.

<http://hdl.handle.net/10945/17031>

Downloaded from NPS Archive: Calhoun



<http://www.nps.edu/library>

Calhoun is the Naval Postgraduate School's public access digital repository for research materials and institutional publications created by the NPS community. Calhoun is named for Professor of Mathematics Guy K. Calhoun, NPS's first appointed -- and published -- scholarly author.

Dudley Knox Library / Naval Postgraduate School
411 Dyer Road / 1 University Circle
Monterey, California USA 93943

FORMULATION AND COMPARISON OF
INSTANTANEOUS DISTORTION INDICES
FOR ASSESSING COMPRESSOR STALL

John Lloyd Vann

KNOX LIBRARY
POSTGRADUATE SCHOOL
PASADENA, CALIFORNIA 93946

NAVAL POSTGRADUATE SCHOOL

Monterey, California



THESIS

FORMULATION AND COMPARISON OF
INSTANTANEOUS DISTORTION INDICES
FOR ASSESSING COMPRESSOR STALL

by

John Lloyd Vann

June 1974

Thesis Advisor:

Allen E. Fuhs

Approved for public release; distribution unlimited.

+ 162487

REPORT DOCUMENTATION PAGE		READ INSTRUCTIONS BEFORE COMPLETING FORM
1. REPORT NUMBER	2. GOVT ACCESSION NO.	3. RECIPIENT'S CATALOG NUMBER
4. TITLE (and Subtitle) FORMULATION AND COMPARISON OF INSTANTANEOUS DISTORTION INDICES FOR ASSESSING COMPRESSOR STALL		5. TYPE OF REPORT & PERIOD COVERED Master's Thesis June 1974
7. AUTHOR(s) John Lloyd Vann		6. PERFORMING ORG. REPORT NUMBER
9. PERFORMING ORGANIZATION NAME AND ADDRESS Naval Postgraduate School Monterey, California 93940		8. CONTRACT OR GRANT NUMBER(s)
11. CONTROLLING OFFICE NAME AND ADDRESS Naval Postgraduate School Monterey, California 93940		10. PROGRAM ELEMENT, PROJECT, TASK AREA & WORK UNIT NUMBERS
14. MONITORING AGENCY NAME & ADDRESS (if different from Controlling Office) Naval Postgraduate School Monterey, California 93940		12. REPORT DATE June 1974
		13. NUMBER OF PAGES 102
		15. SECURITY CLASS. (of this report) Unclassified
16. DISTRIBUTION STATEMENT (of this Report) Approved for public release; distribution unlimited.		15a. DECLASSIFICATION/DOWNGRADING SCHEDULE
17. DISTRIBUTION STATEMENT (of the abstract entered in Block 20, if different from Report)		
18. SUPPLEMENTARY NOTES		
19. KEY WORDS (Continue on reverse side if necessary and identify by block number) Vorticity; Compressor Stall; Distortion Index; Instantaneous Distortion Indices		
20. ABSTRACT (Continue on reverse side if necessary and identify by block number) This thesis examines the problem of predicting distortion induced stall in an axial flow compressor. Three instantaneous distortion indices are used on the data presented. The data consist of eleven stall events run at 2.5 Mach by NASA Lewis on a J85-GE-13 turbojet engine. The three indices used include two indices based on vorticity and developed at the Naval Postgraduate School. The third index was developed		

Block 20 - ABSTRACT (Cont.)

by Pratt and Whitney and is based on total pressure distributions. The three indices are compared by visual means using computer plots and are also compared by using a simple statistical approach. The computer program used was first developed by Shoemaker in his Master's thesis. The program is expanded in this thesis to compute and compare the three indices.

Formulation and Comparison of
Instantaneous Distortion Indices
for Assessing Compressor Stall

by

John Lloyd Yann
Lieutenant, United States Navy
B.S., Naval Postgraduate School, 1973

Submitted in partial fulfillment of the
requirements for the degree of

MASTER OF SCIENCE IN AERONAUTICAL ENGINEERING

from the

NAVAL POSTGRADUATE SCHOOL
June 1974

ABSTRACT

This thesis examines the problem of predicting distortion induced stall in an axial flow compressor. Three instantaneous distortion indices are used on the data presented. The data consist of eleven stall events run at 2.5 Mach by NASA Lewis on a J85-GE-13 turbojet engine. The three indices used include two indices based on vorticity and developed at the Naval Postgraduate School. The third index was developed by Pratt and Whitney and is based on total pressure distributions. The three indices are compared by visual means using computer plots and are also compared by using a simple statistical approach. The computer program used was first developed by Shoemaker in his Master's thesis. The program is expanded in this thesis to compute and compare the three indices.

TABLE OF CONTENTS

I.	INTRODUCTION -----	10
II.	NATURE OF THE PROBLEM -----	12
	A. COMPRESSOR SURGE -----	12
	B. CLEAN STALL VERSUS DISTORTION INDUCED STALL ---	15
III.	DISTORTION INDICES -----	17
	A. VORTICITY VIA CROCCO'S THEOREM -----	17
	B. SHOEMAKER INDEX -----	18
	C. DOWNS INDEX -----	20
	D. PRATT AND WHITNEY K_{DM} DISTORTION INDEX -----	22
IV.	EXPLANATION OF DATA -----	24
V.	THREE INDICES APPLIED TO DATA -----	29
	A. EXAMINATION PROCEDURE -----	29
	B. COMPARISON OF RESULTS -----	31
VI.	CONCLUSIONS -----	35
	APPENDIX A COMPUTER PLOTS -----	37
	COMPUTER OUTPUT -----	71
	COMPUTER PROGRAM -----	80
	LIST OF REFERENCES -----	96
	INITIAL DISTRIBUTION LIST -----	97

LIST OF TABLES

I.	Steady-State Operating Conditions -----	26
II.	Explanation of Program Terms -----	30
III.	Computer Plot Summary -----	32
IV.	Statistical Summary -----	33

LIST OF FIGURES

1.	Compressor Characteristics -----	13
2.	Velocity Diagram -----	13
3.	Compressor-Throttle System -----	14
4.	Characteristics Plot -----	14
5.	Rotating Stall -----	16
6.	Effect of Pressure and Radial Vorticity on β -----	21
7.	Compressor Face -----	27
A-1	Shoemaker Index case one -----	38
A-2	Downs Index case one -----	39
A-3	Pratt and Whitney Index case one -----	40
A-4	Shoemaker Index case two -----	41
A-5	Downs Index case two -----	42
A-6	Pratt and Whitney Index case two -----	43
A-7	Shoemaker Index case three -----	44
A-8	Downs Index case three -----	45
A-9	Pratt and Whitney Index case three -----	46
A-10	Shoemaker Index case four -----	47
A-11	Downs Index case four -----	48
A-12	Pratt and Whitney Index case four -----	49
A-13	Shoemaker Index case five -----	50
A-14	Downs Index case five -----	51
A-15	Pratt and Whitney Index case five -----	52
A-16	Shoemaker Index case six -----	53
A-17	Downs Index case six -----	54
A-18	Pratt and Whitney Index case six -----	55

A-19	Shoemaker Index case seven -----	56
A-20	Downs Index case seven -----	57
A-21	Pratt and Whitney Index case seven -----	58
A-22	Shoemaker Index case eight -----	59
A-23	Downs Index case eight -----	60
A-24	Pratt and Whitney Index case eight -----	61
A-25	Shoemaker Index case nine -----	62
A-26	Downs Index case nine -----	63
A-27	Pratt and Whitney Index case nine -----	64
A-28	Shoemaker Index case ten -----	65
A-29	Downs Index case ten -----	66
A-30	Pratt and Whitney Index case ten -----	67
A-31	Shoemaker Index case eleven -----	68
A-32	Downs Index case eleven -----	69
A-33	Pratt and Whitney Index case eleven -----	70

ACKNOWLEDGEMENT

The author wishes to thank Professor Allen E. Fuhs of the Naval Postgraduate School at Monterey Calif. His endless flow of ideas, professional guidance, and refreshing sense of humor have truly made this thesis possible.

The author also wishes to thank Mr. Paul Burstadt of the NASA Lewis Research Center in Cleveland, Ohio. Mr. Burstadt has certainly gone out of his way to provide information and data for the preparation of this thesis.

I. INTRODUCTION

This paper addresses the problem of distortion-induced or drift stall in an axial flow compressor. The problem is a current one in industry and has not been wholly resolved. The present method of dealing with the problem of distortion is to operate axial flow compressors with a sufficient stall margin to avoid the problem altogether, but this is an expensive procedure. Best engine efficiencies are obtained by operating close to the stall or surge line. By providing a large stall margin, we are in effect sacrificing performance via reduced efficiencies. The problem is especially germane to military aircraft. The normal operating conditions of military aircraft include hard maneuvering, high "g" flight, steam ingestion from aircraft carrier launches, and exhaust gas ingestion from forward firing weapons. These operating regimes cause a pressure, temperature, and gaseous molecular weight distortion of the flow entering the compressor section of the engine.

In order to deal with distortion, it is first necessary to find or define an adequate measure of it. A distortion index based on steady-state or long-time averaged values of distortion has been attempted. This method has met with some degree of success, but it is apparent that peak instantaneous distortions of sufficient magnitude can induce stall when the time averaged distortion factor remains relatively low. The current approach and the approach of this paper is to

examine distortion as an unsteady phenomenon and to measure distortion over time intervals comparable with the characteristic times of an axial compressor.

A computer program was first developed by Ens. Shoemaker [ref 3] utilizing an existing interpolation scheme developed at the Lewis Research Center of NASA. The program calculates the total pressure distribution just prior to the compressor section of a J85-GE-13 turbojet engine as a function of time. The program also utilizes the theory of Fuhs, Farmer, and Iverson [ref 1, ref 2] to compute the circumferential and radial components of vorticity across the face of the compressor section as a function of time. The computer program was extended for this paper to calculate and statistically compare two existing distortion indices plus an additional index developed by Downs and studied in this thesis [ref 4]. This procedure was applied to eleven stall events recorded and analyzed by the NASA Lewis Research Center [ref 5].

II. NATURE OF THE PROBLEM

A. COMPRESSOR SURGE

The line marked "surge" in figure 1 denotes the locus of unstable operation points for an axial compressor. The cause of compressor surge may be visualized in the following manner. At any given reference RPM ($N/\sqrt{\theta}$) and blade radius, a rotor speed U is specified. Consider the velocity diagram in figure 2. A reduction in referred mass flow rate will cause a reduction in the axial component of velocity. Since the rotor speed is fixed, an increase in the relative flow angle β will occur. Present compressor design incorporates a fixed rotor geometry and thus the relative flow angle may only increase to a maximum value which is dependent on blade design.

An insight into the unstable nature of the surge line may be made by comparing the characteristics of the compressor to the characteristics of a throttle. A throttle is set to produce a certain back or receiver pressure, given an inlet pressure. We may visualize a system consisting of a compressor producing a high inlet pressure followed by a throttle which dumps the high compressor air to ambient conditions (fig 3). A plot of the characteristics of the hypothetical throttle and compressor are included in figure 4. The compressor is represented at a fixed reference RPM. The dashed lines represent fixed throttle settings. Selecting a particular throttle setting determines two possible

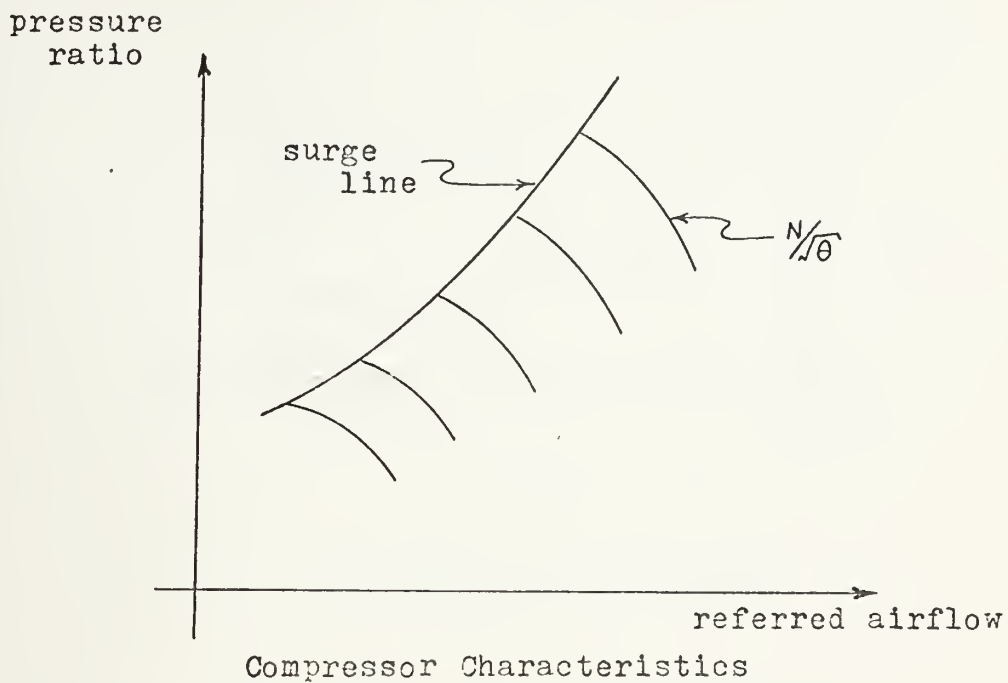


FIGURE 1

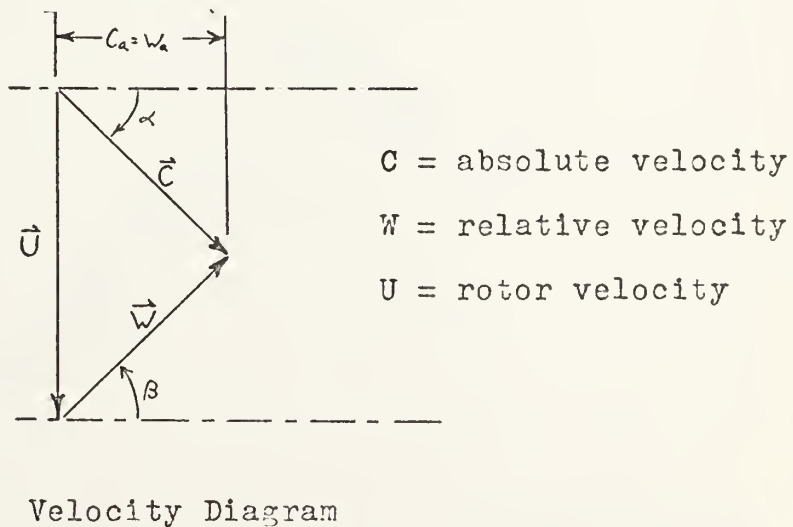
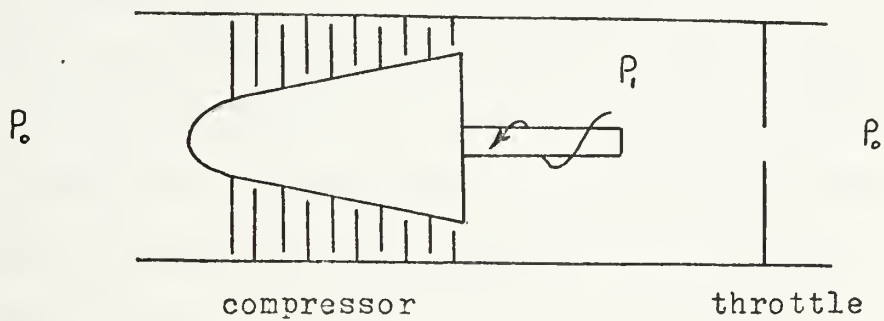
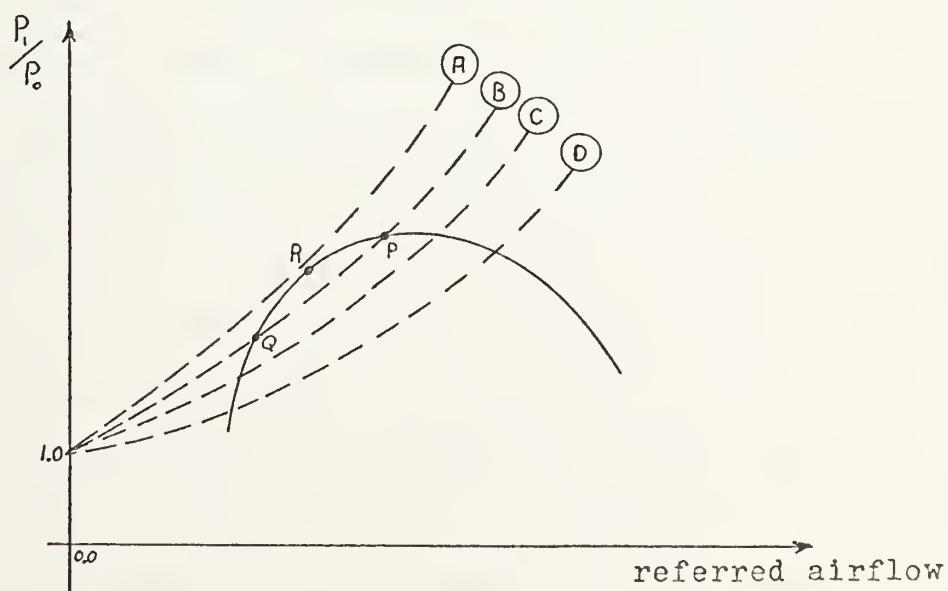


FIGURE 2



Compressor-Throttle System

FIGURE 3



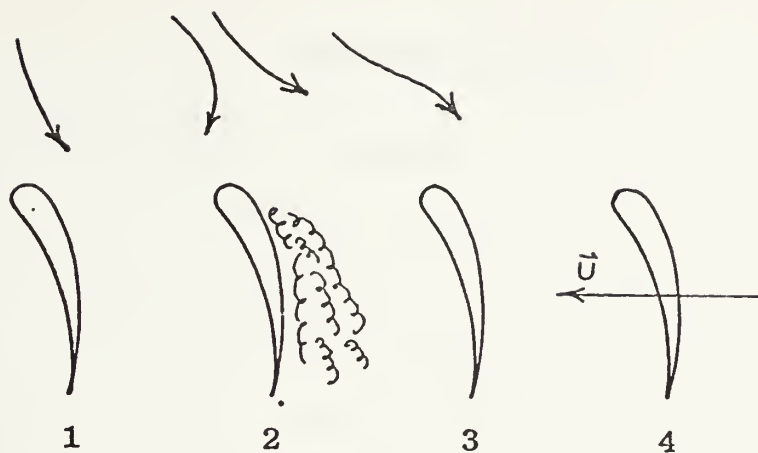
Characteristics Plot

FIGURE 4

compressor points. Consider as a throttle setting line B, with possible operating points P and Q. First consider point P. If the mass flow rate is perturbed to a higher mass flow rate, the throttle setting will demand a higher pressure ratio, whereas the compressor produces a lower pressure ratio. In this case the combination of compressor and throttle will return to point P. Conversely a lower flow rate will cause the throttle to demand a lower pressure ratio whereas the compressor will produce a higher ratio. Again the system will be forced to return to point P. Consider now point Q. A slight perturbation mass flow will produce problems. The system is free in this case to follow any perturbations and the system is unstable. Neutral stability is represented by point R where the slope of the throttle curve matches the slope of the compressor curve.

B. CLEAN STALL VERSUS DISTORTION INDUCED STALL

The surge line in figure 1 denotes the conditions at which stall will occur if the inlet velocity profile is uniform, producing a uniform total pressure distribution. In actuality, the velocity profile is not uniform and pressure perturbations may produce a local condition over a small region of the compressor face which will cause stall over that region. This stalled region in turn produces a condition known as rotating stall. In figure 5, if the conditions are such that blade 2 becomes stalled, the effective flow area between blades 2 and 3 is reduced. This reduction in flow



Rotating Stall

FIGURE 5

area causes a flow diversion which tends to overload and stall blade 3. Continuation of this process will produce rotating stall. It is noteworthy that rotating stall propagates in the opposite direction from rotor velocity at about half rotor speed. Rotating stall may develop into surge or fully developed stall.

It is apparent that the instantaneous velocity distributions across the compressor face may cause stall when the steady-state conditions are below the surge line. This velocity distribution in turn produces a total pressure distribution which is the form of the data examined in this thesis.

III. DISTORTION INDICES

A. VORTICITY VIA CROCCO'S THEOREM

Non-dimensional vorticity components in both the circumferential and radial directions of a cylindrical coordinate system may be calculated using the theory of Fuhs, Farmer and Iverson [ref 1, ref 2]. Starting with Crocco's Theorem and using an order of magnitude analysis, it was possible to reduce the expression for these parameters to:

$$\omega'_{\theta} = \frac{-1}{\gamma P' U'_Z} \frac{\partial P'}{\partial r'} - \frac{M}{2} \frac{\partial T'}{\partial r'} ; \quad \omega'_r = \frac{1}{\gamma P' r' U'_Z} \frac{\partial P'}{\partial \theta} + \frac{M}{2 r'} \frac{\partial T'}{\partial \theta}$$

where:

$$P' = \frac{P_T}{\bar{P}_T} ; \quad \omega'_{\theta} = \frac{\omega_{\theta} D}{2 \bar{a}} ; \quad r' = \frac{2r}{D} ; \quad U'_Z = \frac{U_Z}{\bar{a}} ; \quad T' = \frac{T_T}{\bar{T}_T}$$

For a detailed explanation, consult reference 1. The calculations are examined more briefly in reference 2.

Analytical studies and data analysis have been performed in an attempt to relate the effects of total temperature and total pressure distortions on compressor performance [ref 7]. The vorticity approach is well suited to this problem, as both total temperature and total pressure may be taken into account in the calculations of vorticity. It would be beneficial to examine data which consist of both temperature and pressure patterns across the compressor face. Additional work in this area would be helpful. The data examined in this thesis, however, did not present a significant temperature gradient and the expressions for vorticity could be

reduced to:

$$\omega'_{\theta} = \frac{-1}{\gamma P' U'_z} \frac{\partial P'}{\partial r'} ; \quad \omega'_r = \frac{1}{\gamma P' r' U'_z} \frac{\partial P'}{\partial \theta}$$

The task of this thesis was to determine whether an index based on vorticity would provide a meaningful prediction of compressor stall. Two such indices based on vorticity are examined in this thesis. The first index was proposed by Shoemaker [ref 3] and is based on circumferential vorticity. A second index proposed by Downs [ref 4] and based on both radial vorticity and total pressure is examined. In order to provide a means of comparison, a third index based on total pressure and taken from Zonars [ref 8] was also examined.

B. SHOEMAKER INDEX

James E. Shoemaker approached the problem of finding a vorticity based index by first printing out maps of pressure, circumferential vorticity and radial vorticity. In order to accomplish this goal he utilized a set of subroutines developed at Wright Patterson Air Force Base, and altered them to print out the maps at times near stall and at times far from stall, to provide a comparison. A copy of his computer program is included at the end of his Master's thesis [ref 3]. Using this procedure, Shoemaker found a vorticity pattern that frequently occurred within twenty-five milliseconds of stall, and was not common at other times. The pattern was characterized by a ring of large negative circumferential vorticity at the midspan of the compressor face, and a large positive ring at the tip. He developed an index based on

this pattern which will be referred to as the Shoemaker index. He divided the compressor face into three concentric regions. Region one at r' less than 0.5 was ignored. Region II was established as that area between radii of 0.55 and 0.70. Region III was that area between radii of 0.8 and 0.95. The Shoemaker index then summed over Region II but set any positive circumferential vorticity equal to zero. Likewise Region III was summed where any negative vorticity was set equal to zero. The instantaneous Shoemaker index was set equal to the sum of the absolute value of the two summations. In notation form,

$$\text{Shoemaker Index (T)} = \frac{1}{N} \sum [\omega_{\theta}^{+}] - \frac{1}{N} \sum [\omega_{\theta}^{-}]$$

where ω_{θ}^{+} = positive values of circumferential vorticity in
Region III

ω_{θ}^{-} = negative values of circumferential vorticity in
Region II

In order to take into account the added effect of the duration of the pattern, Shoemaker set his final index equal to the product of three consecutive instantaneous indices described above. This latter procedure was not used in the present thesis. The Shoemaker index as used herein thus refers to the instantaneous index and is an indication of distortion in the radial direction.

The Shoemaker index has one real advantage when the transport time from the measuring probes to the compressor stage (where stall originates) is considered. The pattern

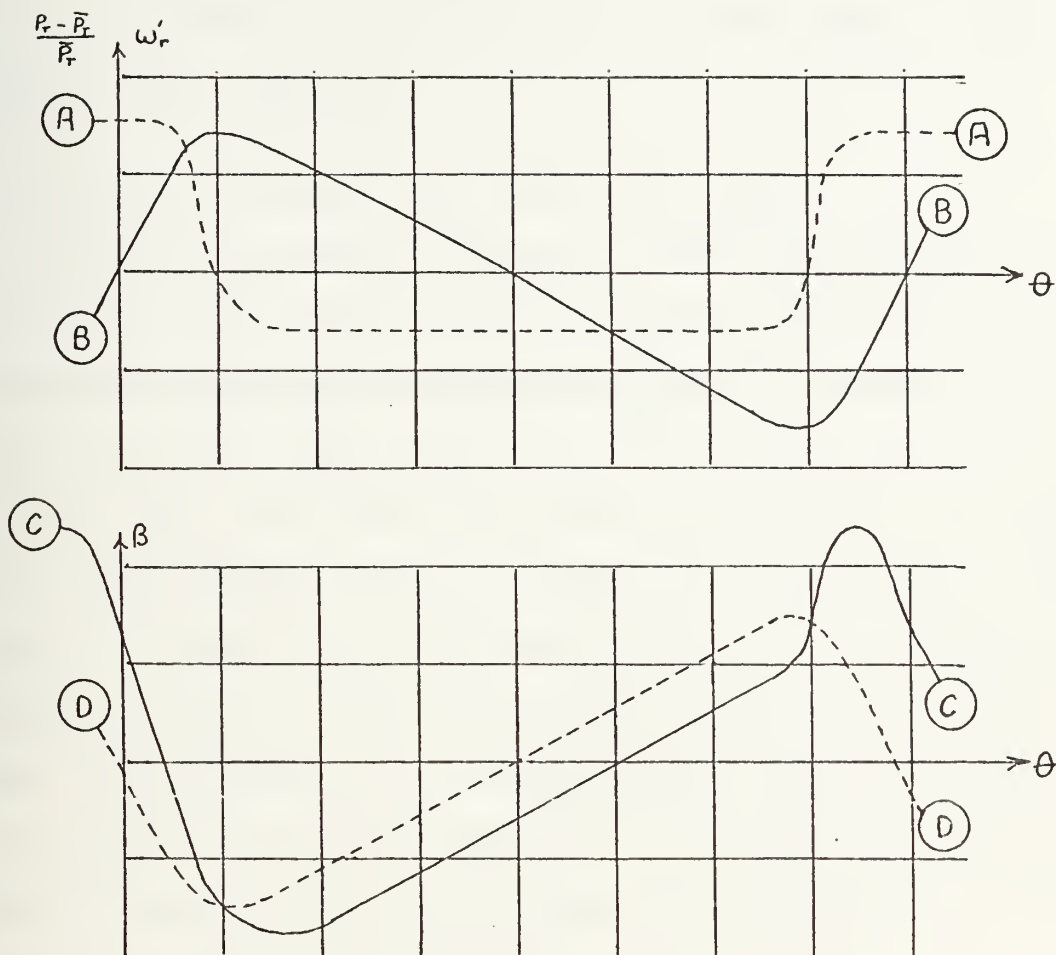
develops at a time before stall which is larger than the transport time from the measuring probes to the stall region. This could be very useful if variable stators or the fuel control were available to avert stall.

C. DOWNS INDEX

A second index which was proposed by Downs [ref 4] was formulated and is explored in this thesis. This index incorporates both total pressure and radial vorticity. The basic idea was to consider the contribution of both total pressure and vorticity to the relative flow angle β . Increasing β would cause the rotor blade incidence angle to increase and would tend to load the blade. A perturbation plot of β versus θ , where the deviation of β from the reference line takes into account pressure and vorticity effects, is shown in figure 6. The corresponding plot of total pressure and ω'_r is also shown. The reference line represents uniform flow. It can be seen that although ω'_r is dependent upon the pressure gradient, the combined effect of pressure and ω'_r on β is dependent on both the gradient and relative magnitude of pressure. The Downs index was formulated to search the compressor face for the largest value of the combined effect of pressure plus ω'_r over any 60 degree sector. In notation form,

$$\text{Downs Index (t)} = \Sigma \left[\frac{\bar{P}_T - P_T}{\bar{P}_T} + \omega'_r \right]_{\max 60}$$

where \bar{P}_T = average total pressure over entire face of compressor at time t



A = possible ω'_r

B = corresponding $\frac{P_r - \bar{P}_r}{\bar{P}_r}$

C = $\frac{P_r - \bar{P}_r}{\bar{P}_r}$ plus ω'_r effect on β

D = $\frac{P_r - \bar{P}_r}{\bar{P}_r}$ effect on β

θ measured in direction of rotor rotation

Effect of pressure and radial vorticity on β

FIGURE 6

The Downs index is primarily an indication of distortion in the circumferential direction. For a more complete analysis, consult Downs [ref 4].

D. PRATT AND WHITNEY K_{DM} DISTORTION INDEX

In order to provide a means of comparison between vorticity based indices and an index calculated directly from total pressures, the Pratt and Whitney K_{DM} index was selected from Zonars [ref 8]. This index was selected primarily because of case four, which was one of the eleven cases investigated. Distortion indices are plotted for all eleven cases in Appendix A. Neither of the vorticity indices had satisfactorily predicted stall in case four; from examining the pressure maps, K_{DM} appeared to be an appropriate index. The K_{DM} index was applied to case four and to all other cases. This index was developed by Pratt and Whitney for the TF-30 installed in the F-111A aircraft and is defined as follows:

$$K_{DM} = \frac{\frac{1}{2} \sum \left[\frac{P_{Tmax} - P_{Tmin}}{P_{Tave}} \right]_i \theta_i^- C_i}{\sum C_i} \times 100$$

where C = ratio of compressor inlet radius to ring radius

i = number of ring

θ^- = largest continuous arc of the ring over which
the total pressure is below the ring average
pressure

P_{Tmax} = ring maximum total pressure

P_{Tave} = ring average total pressure

P_{Tmin} = ring minimum total pressure

It can be seen that the K_{DM} index is an indication of distortion in the circumferential direction and puts more emphasis on the region near the hub. It would be expected that the K_{DM} index and the Downs index would be comparable since both search for circumferential distortion. This was in fact the case and will be discussed in a later section.

IV. EXPLANATION OF DATA

The NASA Lewis Research Center conducted an experimental wind-tunnel investigation to determine the effects of time-varying total-pressure distortions produced in a supersonic inlet on a J85-GE-13 turbojet engine [ref 5]. Selected data taken during this investigation were digitized on magnetic tape; the latter is the source of data used in this thesis. The following explanation of data is largely a brief summary of the explanation presented by Burstadt and Calogeras [ref 5] and is given here to provide an overall understanding of the data analysis.

The inlet was an axisymmetric mixed-compression type. The compressor was an eight-stage axial flow compressor with interstage bleed and variable inlet guide vanes. An after-burner section was present but was not used during the test procedure. The engine bleed system was modified to make the compressor operate with less than normal stall margin. The following excerpt is quoted from reference 5:

The test procedure was to establish an engine operating condition in the vicinity of the compressor stall point. The FM tape recorder was started and a steady-state data scan was made. Then, while the FM tape recorder was still running, the compressor pressure ratio was increased slightly and the throttle adjusted to maintain a constant rotor speed. If stall did not occur, this procedure was repeated until the stall event was recorded on the FM tape. In some cases the stall occurred after the engine had stabilized at an equilibrium operating condition. These were called 'drift' stalls.

All eleven of the stalls examined in this thesis were of the "drift" type. NASA Lewis considered only seven of the eleven cases in their analysis. Cases 6, 8, 9, and 10 were excluded on the grounds either that their causes were attributable to steady-state distortion levels or that they showed very little loss in stall margin. Table I shows steady-state operating conditions for all eleven cases presented in this thesis. The NASA Lewis analysis identifies each case number as a steady-state reading number. These NASA identifying numbers are included in Table I for comparison [ref 5].

Steady-state and dynamic pressure instrumentation at the compressor face is shown in figure 7. Only the fluctuating component of pressure was recorded from each of the dynamic probes. Absolute pressures were later obtained by adding the fluctuating component to the steady-state value.

Frequency response of the dynamic probes was flat to about 2000 hertz. The fluctuating signal from each pressure transducer was recorded on FM multiplexed tape at 152.4 centimeters per second. The data in a 225 millisecond period just prior to stall were digitized at an effective rate of 8000 points per second per channel. These data when processed by the computer program listed in the back of this thesis provided the distribution of total pressure across the compressor face with a time spacing of 0.125 milliseconds between distributions. The distributions of total pressure were further processed to provide distributions of both circumferential and radial vorticity as a function of time. In order to

TABLE I

STEADY-STATE OPERATING CONDITIONS

CASE NO.	NASA IDENT NO.	M ₀	P ₀ (psfa)	$\frac{\bar{P}_3}{\bar{P}_2}$	$\frac{N^*100}{N^*\sqrt{\theta}}$	W _{corr} (lb/sec)	$\frac{\bar{P}_2}{P_0}$	$\frac{\Delta \bar{P}_{rms}}{\bar{P}}$	α (deg.)
1	154	2.50	1968.5	5.240	92.25	38.5	.799	.0691	0
2	162	2.58	1968.4	5.288	92.89	39.5	.769	.0460	5
3	141	2.50	1966.6	7.045	98.82	42.6	.761	.0851	0
4	148	2.50	1966.2	4.601	86.88	34.2	.788	.0658	0
5	164	2.58	1967.4	4.388	86.89	34.9	.843	.0185	5
6	82	2.58	1965.2	4.784	86.34	34.0	.854	.0156	5
7	103	2.68	1972.3	4.684	86.42	33.7	.736	.0500	0
8	200	2.50	1970.5	6.808	95.98	41.0	.768	.0275	0
9	214	2.50	1971.7	5.341	87.29	32.8	.739	.0209	0
10	219	2.50	1958.8	5.812	89.93	35.3	.794	.0167	0
11	261	2.58	1972.5	4.355	87.00	34.8	.783	.0209	6

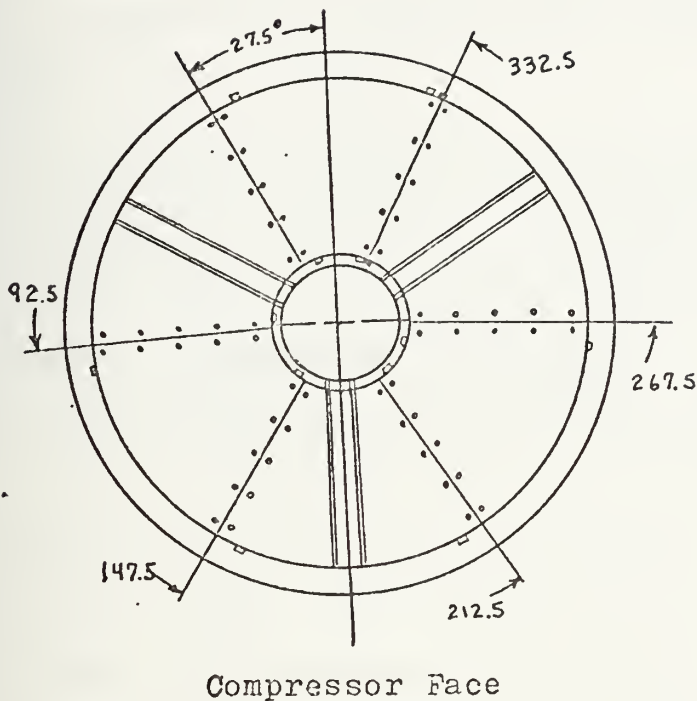


FIGURE 7

TYPE OF PRESSURE

□ STATIC

○ TOTAL

OPEN SYMBOL IMPLIES

STEADY STATE

SOLID SYMBOL IMPLIES

DYNAMIC

reduce the amount of calculating involved, only one out of five readings was actually processed so that there was five times 0.125 or 0.625 milliseconds of time between readings actually processed.

The determination of stall time was made by NASA Lewis. The signals from the compressor static pressure transducers were put on strip charts and examined by NASA. For all cases, the row of instrumentation at the 290 degree location showed the earliest indication of stall. Since the origin of stall in a compressor stage causes an abrupt loss in the airflow pumping of that stage, a compression wave is

propagated upstream. This compression wave is referred to as a hammer shock. The following excerpt is quoted from reference 5:

Because there were only two axial rows of instrumentation inside the compressor, it was not possible to determine exactly when stall originated inside the compressor. Although the first indication was seen at the 290 degree location, a stall zone could originate just past the 45 degree location but not be detected until it rotated past the instrumentation at 290 degrees. Since the stall zone rotated at about half rotor speed (8 msec/rev) there could be as much as a 6-millisecond delay before it was detected at the 290 degree location.

A one-millisecond period for transport time between sensors and stall stage, plus time for blade response, was predicted by NASA. This produces a six-plus-one or seven-millisecond possible time lag between actual initialization of stall and the stall time listed in this thesis.

V. THREE INDICES APPLIED TO DATA

A. EXAMINATION PROCEDURE

The computer program first developed by Shoemaker [ref 3] was adapted to compute each index as a function of time for the entire time interval provided by NASA Lewis. This time interval varied slightly but was generally about 215 milliseconds of data prior to first indication of stall. The DRAW subroutine of the Naval Postgraduate School was used to plot each index. These plots are included in Appendix A and are plots of the instantaneous version of each index. A numerical printout was also provided by the program. A sample numerical printout for the Shoemaker index case one is included at the end of this thesis. Table II provides an explanation of the terms for the numerical printout.

In addition to the computer plots, which may be used to determine if the given index is an accurate predictor of stall, a simple statistical approach was used. After the first fifty values of the index were computed, the mean and standard deviation for those fifty values were obtained. Then, as the next fifty values of the index were computed, the following test was made. If the average of the three previous values of the index at any time exceeded a certain criterion value, the computer program printed out a stall warning with the time in milliseconds of occurrence. The criterion level was set in the following manner:

$$\text{Test} = \text{mean} + 2.5 \times \text{standard-deviation.}$$

TABLE II

EXPLANATION OF PROGRAM TERMS

N	= index number (a function of time).
FACT(N)	= value of instantaneous index at time "N".
DFACT(N)	= average of three previous FACT(N) values.
TIME	= "N" time in milliseconds. Starts at zero for each new case.
PTAVE	= average total pressure over compressor face at time "N".
MEAN	= mean value of FACT(N) for 50 previous values of N, when not zero.
STD-DEV	= standard deviation of FACT(N) for 50 previous values of N, when not zero.

At the end of each 50 values of the index, a new mean and standard-deviation were computed and the test criterion was established for the next 50 values of the index. This simple test was used on all thirty-three runs made, and the results are summarized in the next section. Obviously, the test criterion could be lowered, with resulting greater occurrence of stall prediction, but this would also increase the number of false warnings. The value of test was initially set to predict stall for the K_{DM} index Case three without any false warnings. The test criterion could have been set to an optimum value for each particular index with possible better results but this method was not used. The same test was applied to all cases. The statistical method has the real advantage

of not being subject to interpretation. All thirty-three computer plots are included in this thesis, since they certainly are subject to personal interpretation as to the prediction of compressor stall.

B. COMPARISON OF RESULTS

There are two indicators of the results of the data reduction. First are the computer plots, which provide an eyeball examination of results. A matrix summation of the computer plot results is provided by Table III. The second method was the use of statistical mean and standard-deviation discussed in the preceding section. A matrix summation of the statistical method is provided by Table IV. In both tables, where stall was predicted, the time to stall is given in milliseconds.

There are several points of interest. As had been previously expected, there is some correlation between the K_{DM} index and the Downs index, since both rely on circumferential distortion. Using the statistical method, all of the cases predicted by the K_{DM} index were also predicted by the Downs index. The Downs index predicted two additional cases utilizing this method. Using the computer plot interpretation, the K_{DM} method predicts six cases and the Downs index predicts five, with four predictions common to both indices.

If one were to use a combination of both vorticity based indices, the statistical method would have predicted eight out of the eleven cases presented. Using this method there

TABLE III
COMPUTER PLOT SUMMARY

(based on visual interpretation)

RUN	PRATT & WHITNEY K _{pr} INDEX	SHOEMAKER INDEX	DOWNS INDEX
1	No Prediction	22.5 millisecs	23.0 millisecs
2	3.0 millisecs 3 same magnitude	25.0 millisecs	No Prediction one false peak
3	3.0 millisecs	21.0 millisecs 4 false peaks	6.0 millisecs 2 false peaks
4	4.0 millisecs 2 larger peaks	No Prediction	No Prediction one false peak
5	No Prediction	3.0 millisecs 2 smaller peaks	No Prediction
6	No Prediction	No Prediction	No Prediction
7	No Prediction	No Prediction	No Prediction
8	4.5 millisecs	No Prediction	2.0 millisecs
9	4.0 millisecs one false peak	16.0 millisecs 5 same magnitude	2.0 millisecs
10	4.0 millisecs	No Prediction	2.0 millisecs
11	No Prediction	6.0 millisecs 2 larger peaks	No Prediction
totals	6 Predictions	6 Predictions	5 Predictions

TABLE IV
STATISTICAL SUMMARY

RUN	PRATT & WHITNEY K INDEX	SHOEMAKER INDEX	DOWNS INDEX
1	No Prediction	21.8 millisecs 1 false warning	22.28 millisecs 2 false warnings
2	No Prediction	23.9 millisecs	No Prediction 2 false warnings
3	0.9 millisecs	20.2 millisecs 1 false warning	4.88 millisecs 2 false warnings
4	No Prediction	No Prediction 1 false warning	No Prediction 1 false warning
5	No Prediction	No Prediction	No Prediction
6	No Prediction	No Prediction	No Prediction
7	No Prediction	No Prediction	19.88 millisecs 1 false warning
8	2.88 millisecs	No Prediction 2 false warnings	2.38 millisecs
9	0.4 millisecs	35.8 millisecs 2 false warnings	0.0 millisecs
10	1.62 millisecs	No Prediction 1 false warning	2.33 millisecs 1 false warning
11	No Prediction	11.8 millisecs	No Prediction
totals	4 Predictions	5 Predictions	6 Predictions

would have been seventeen false warnings. The number of false warnings could be reduced by a reduction in the test criterion to a point where no loss in stall prediction would occur.

There could be as much as seven milliseconds of time lag between actual stall time and predicted stall time. This presents a problem since the data could include the effects of the hammershock which occurs after stall, if the time lag is too great. It is certainly no problem to produce an index which will sense the hammershock and the question arises, did the index actually predict stall or were the effects of the hammershock being felt? By examining the numerical printout of average total pressure as a function of time and taking into account the possible seven-millisecond lag time, it was apparent that this could have been a problem in only four cases. These four cases should be held suspect and are cases 3, 8, 9, and 10. It is noteworthy that the Shoemaker index predicted stall in two of these four cases sufficiently far in advance to preclude the problem.

VI. CONCLUSIONS

An investigation into the problem of predicting compressor stall using instantaneous distortion parameters was made. Some success was evidenced by both the statistical method and computer plot interpretation, but it was not possible to predict stall in every case using one or any combination of the indices explored. This seems to indicate that an axial compressor is subject to many instantaneous distortion patterns as well as to steady-state distortion, whereas one index may only search for one category of distortion. If the cause of compressor stall was in every case instantaneous radial distortion over the outer portion of the compressor face, then in every case the Shoemaker index should predict stall. If the cause was in every case circumferential distortion over some arbitrary sixty degree sector then the Downs index would be successful. If the distortion conforms to the ring pattern explored by the Pratt and Whitney index, then that method would succeed. In fact, it seems naive to believe that compressor stall could be predicted in every case using any one index. The indices explored in this thesis and the indices used by industry today may certainly be improved upon, but it is doubtful that any one index will prove to be a panacea.

In spite of the compound nature of compressor stall, instantaneous indices are useful. The Pratt and Whitney index used in this thesis was developed for the F-111A with a

specific inlet-engine combination. It is in that context that distortion parameters would appear most useful - that is, to examine an inlet-engine system for compatibility. The performance of an inlet-engine system which too often experiences one type of distortion pattern may be improved upon; distortion indices would be very useful in isolating a predominant pattern.

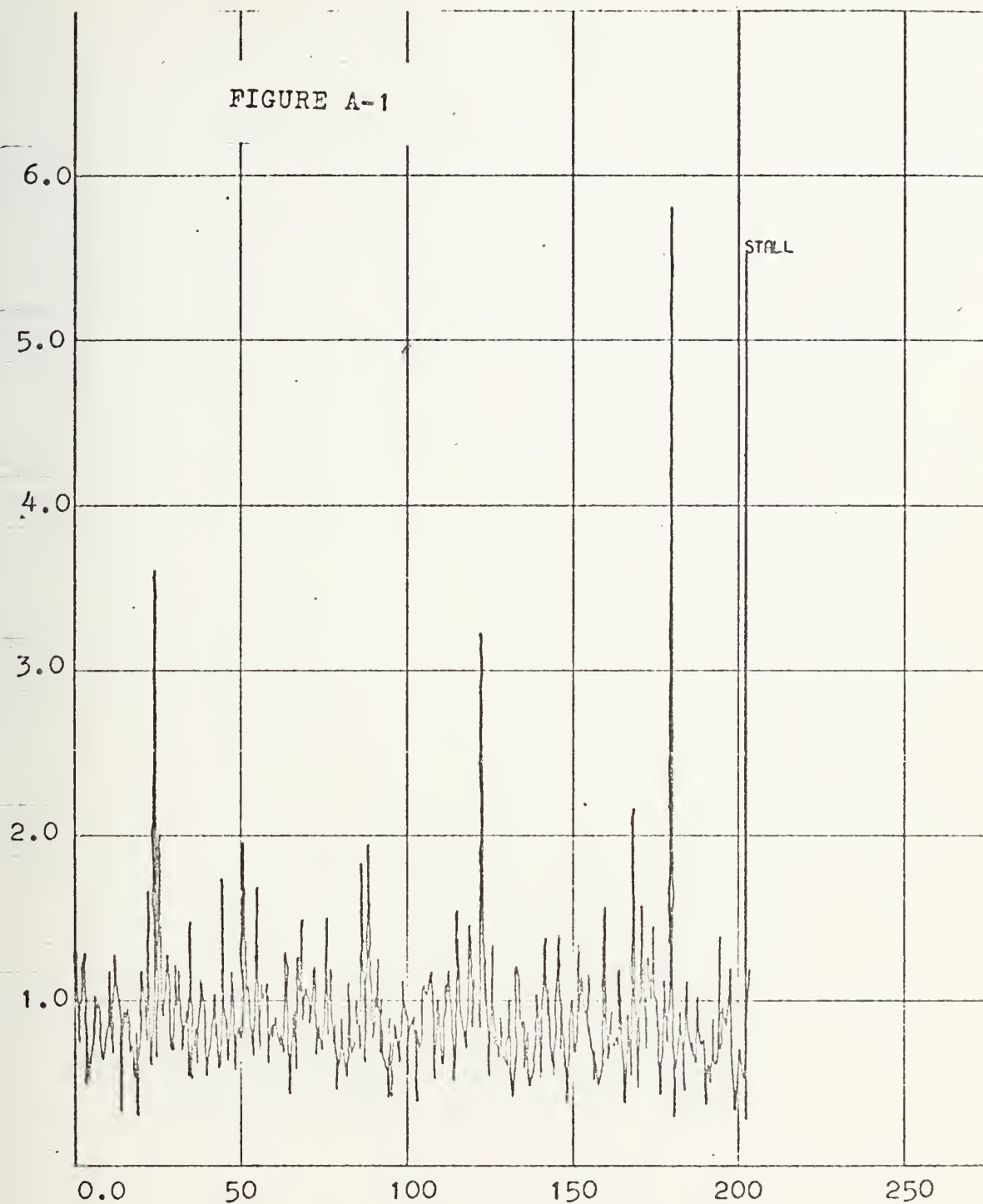
The use of vorticity as an index parameter has some real advantages. Both temperature and pressure gradients may be integrated into a single parameter. Vorticity may be visualized more simply and is a natural characteristic of the fluid. The Shoemaker index, when successful, harbingers stall sufficiently far in advance possibly to enable correction of the deficiency using engine controls. Vorticity appears to be a promising dimensionless parameter and deserves further investigation.

APPENDIX A

COMPUTER PLOTS

The following thirty-three computer plots provide the instantaneous version of each of the three indices considered. In all cases, the horizontal scale is read in milliseconds. The vertical scale gives the index value and is a non-dimensional number. No consideration was given to index magnitude in predicting stall. For any given case, a strong peak just before stall in relation to that particular case was considered to be sufficient for stall prediction.

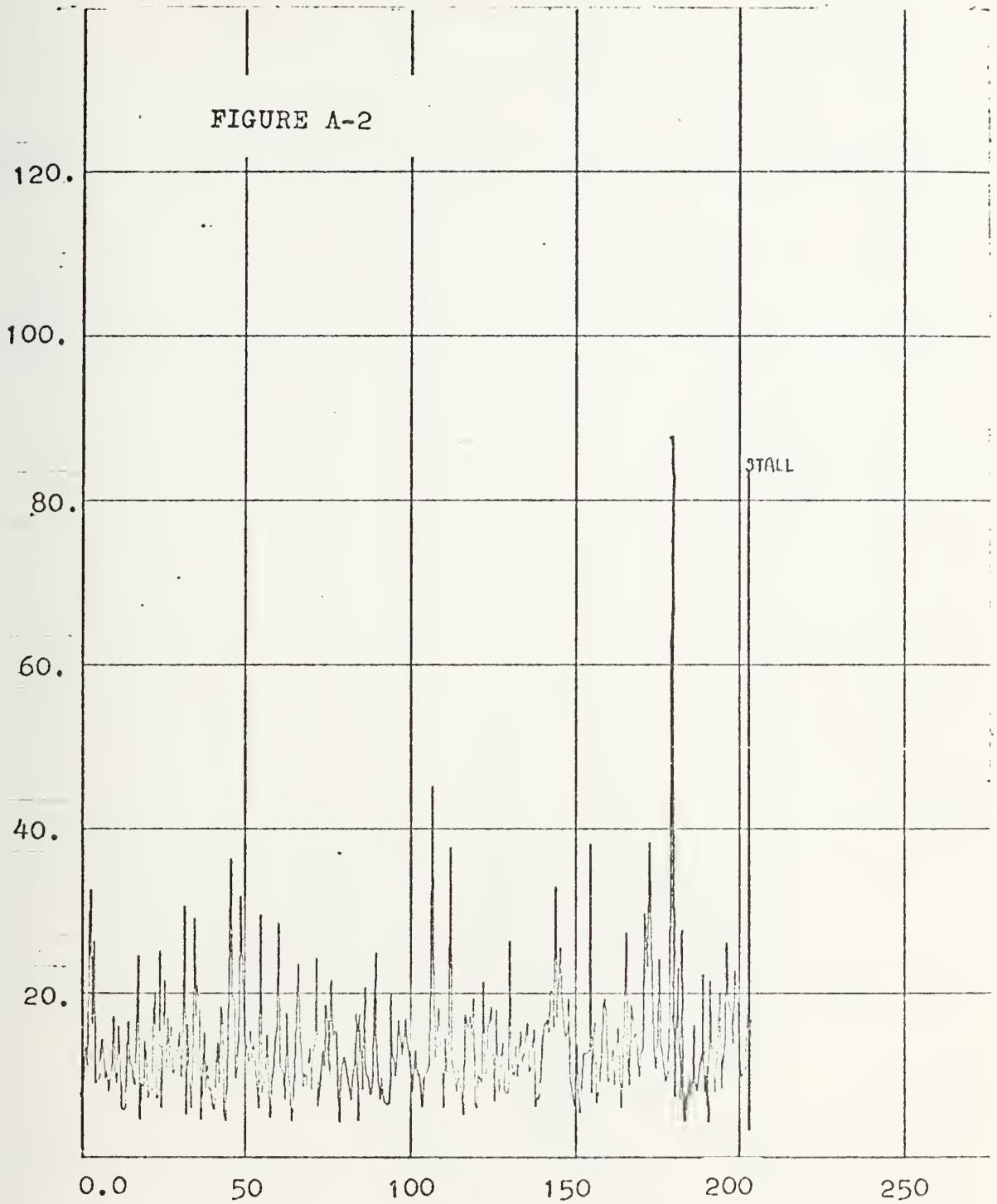
FIGURE A-1



Shoemaker Index

case one

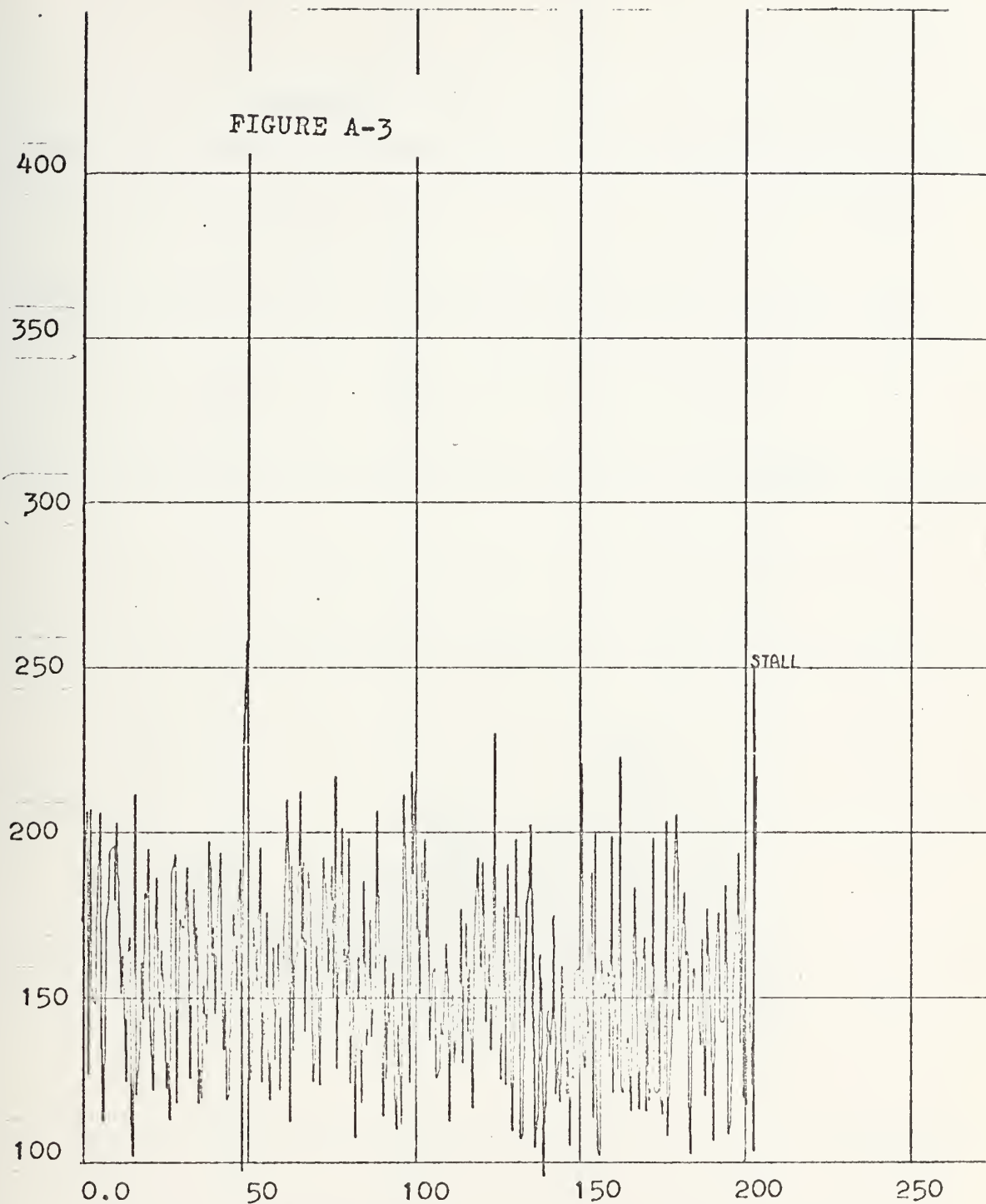
index vs time in millisec



Downs Index

case one

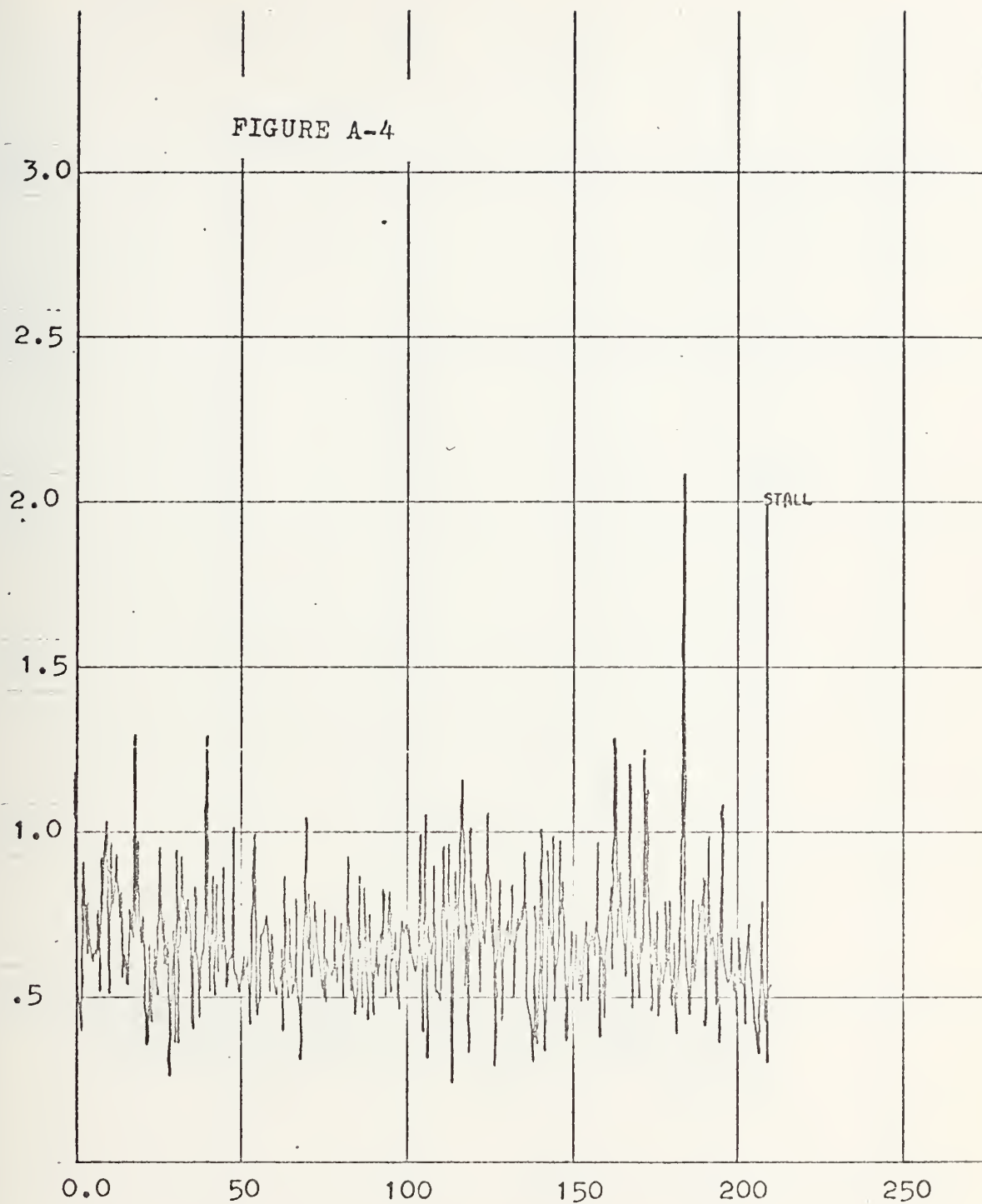
index vs time in millisecc



Pratt and Whitney Index

case one

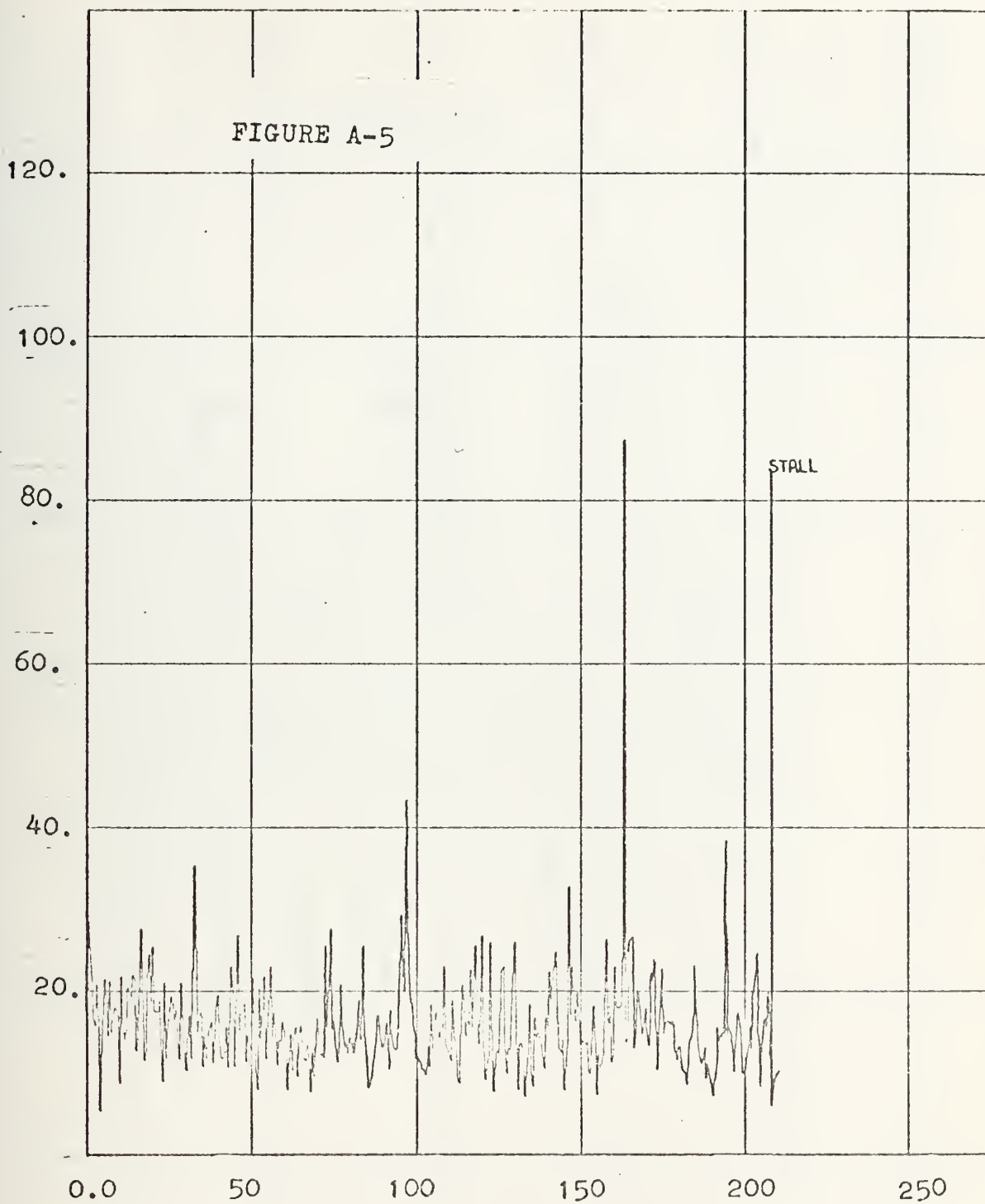
index vs time in millisecc



Shoemaker Index

case two

index vs time in millisecc

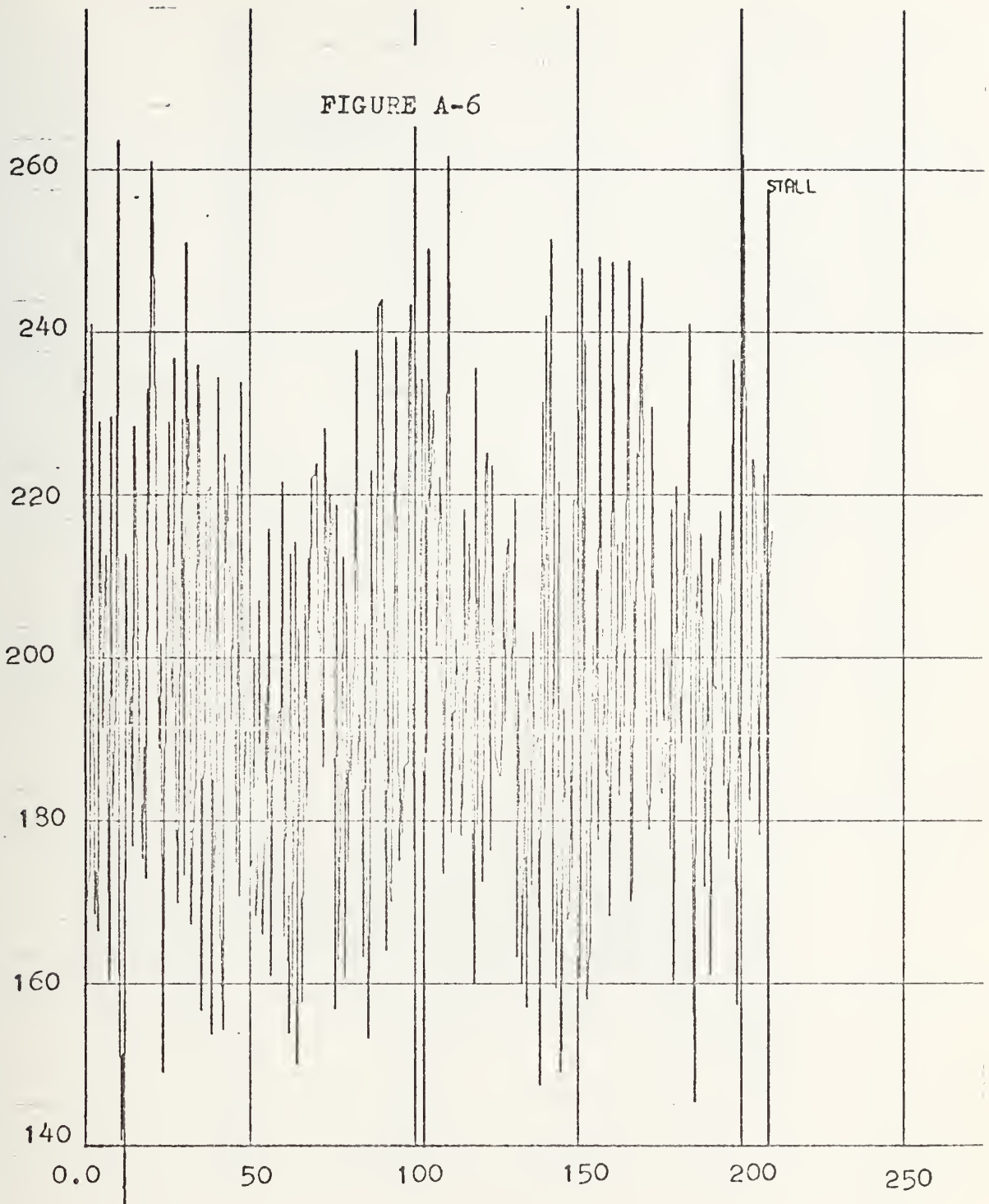


Downs Index

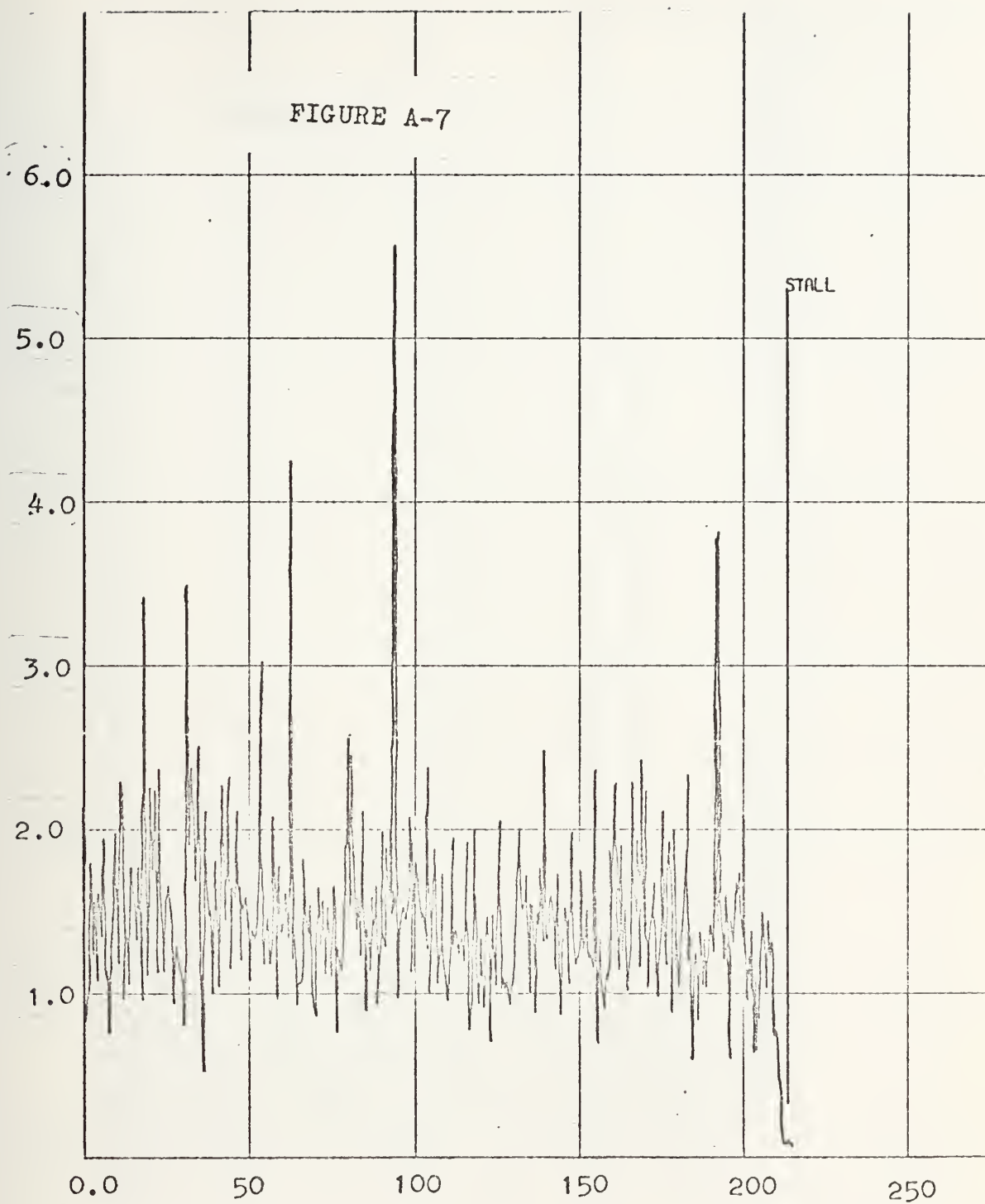
case two

index vs time in millisec

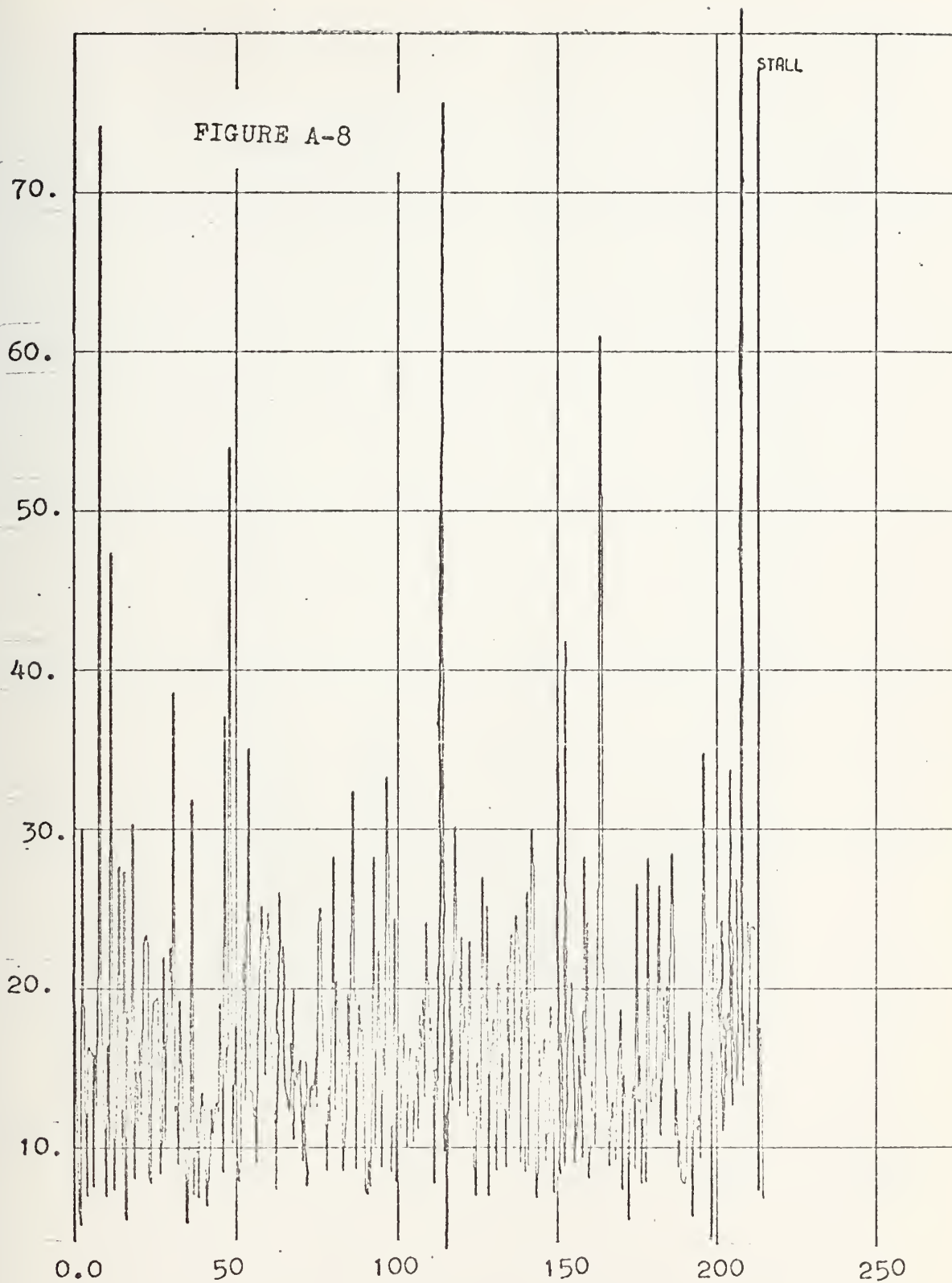
FIGURE A-6



Pratt and Whitney Index
case two
index vs time in millisec



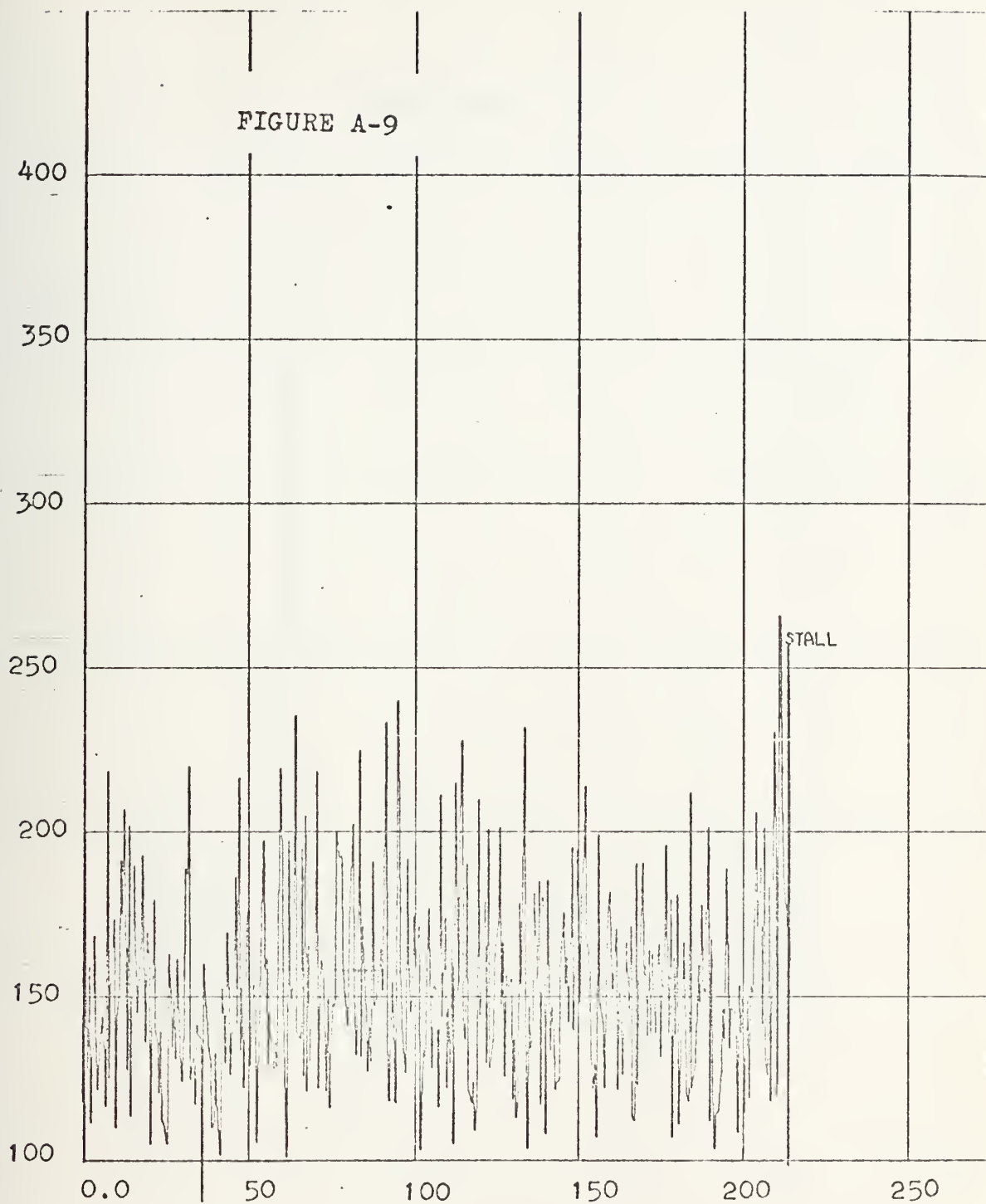
Shoemaker Index
case three
index vs time in millisecc



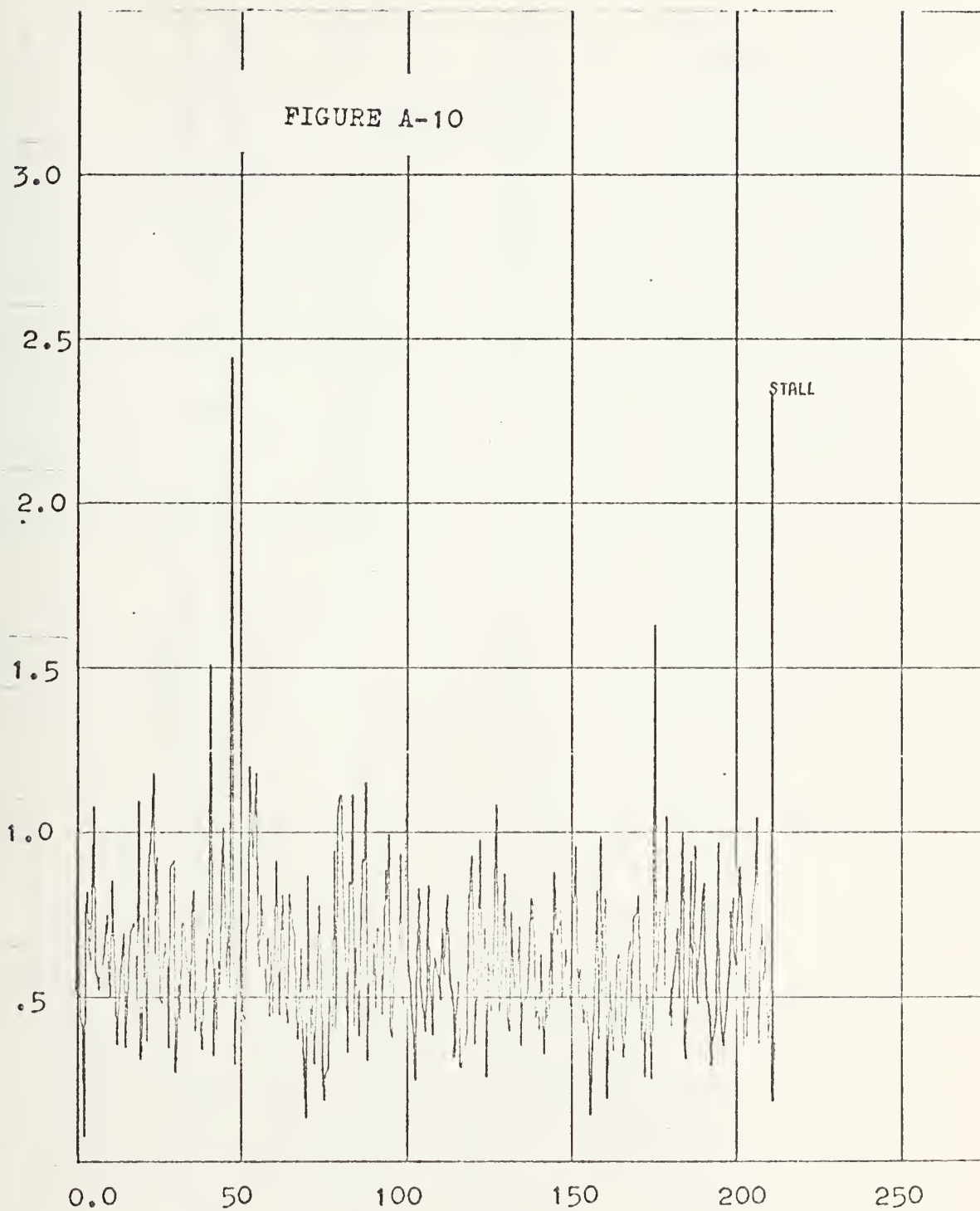
Downs Index

case three

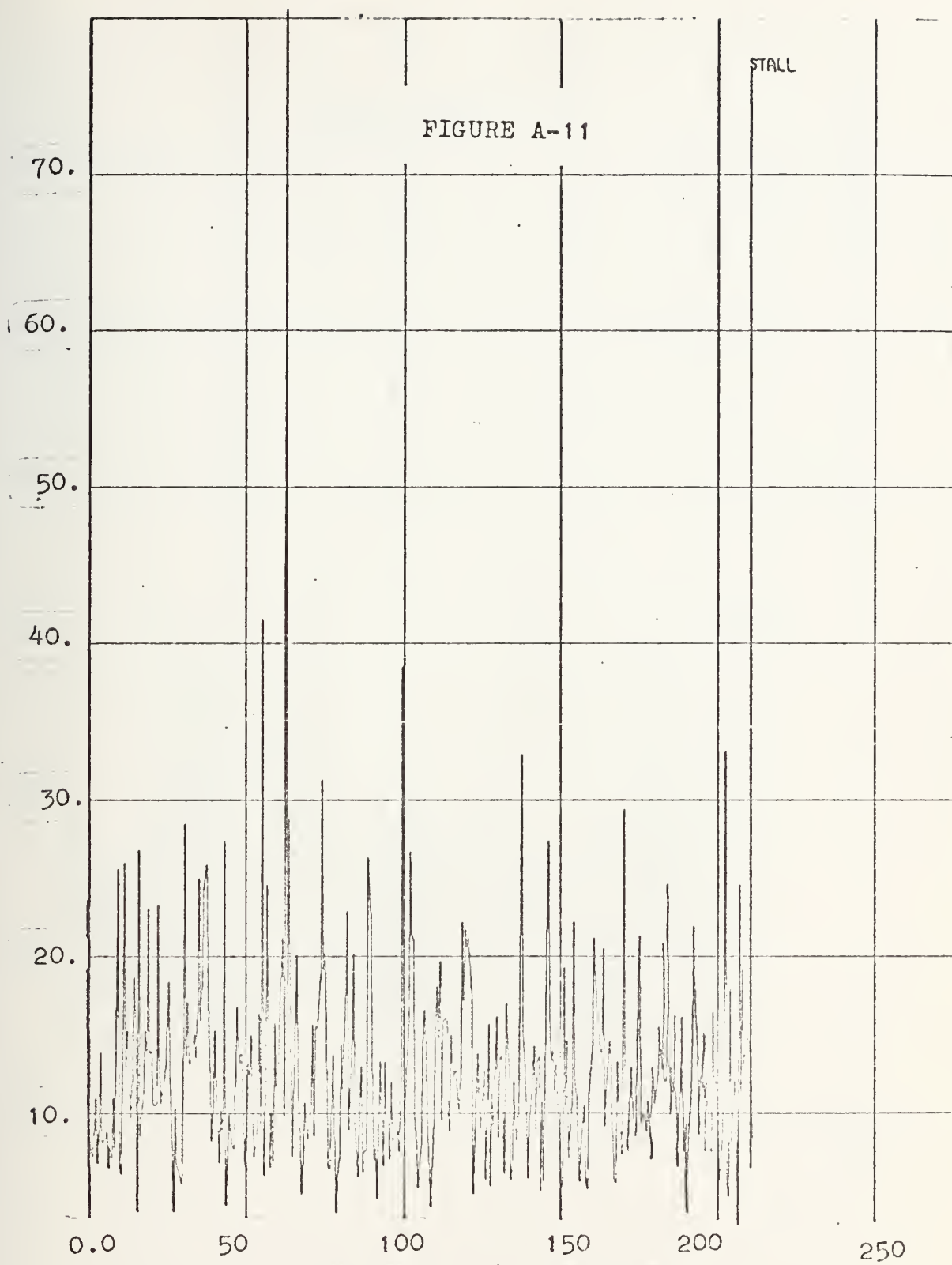
index vs time in millisecc



Pratt and Whitney Index
case three
index vs time in millisec



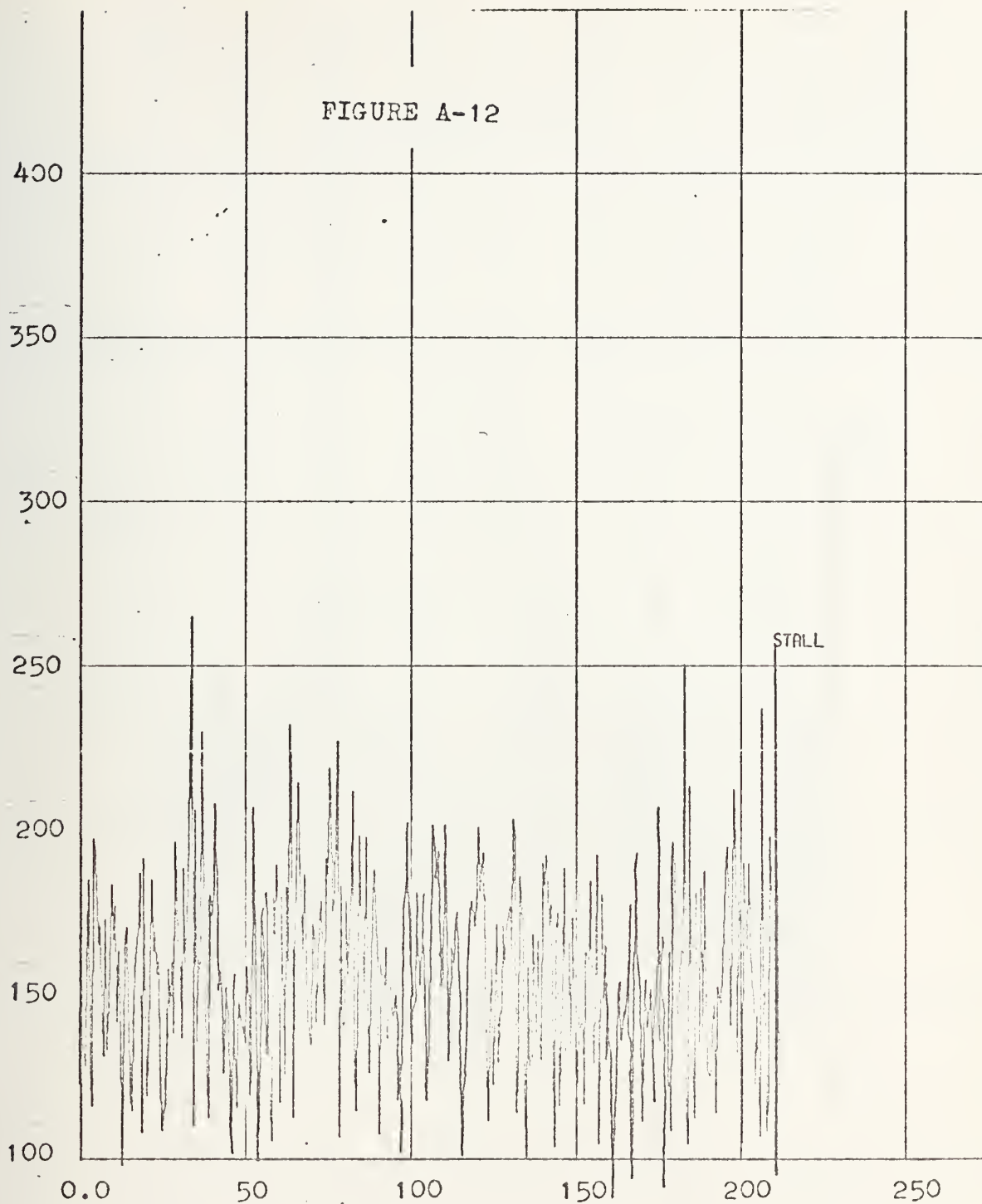
Shoemaker Index
case four
index vs time in millisec



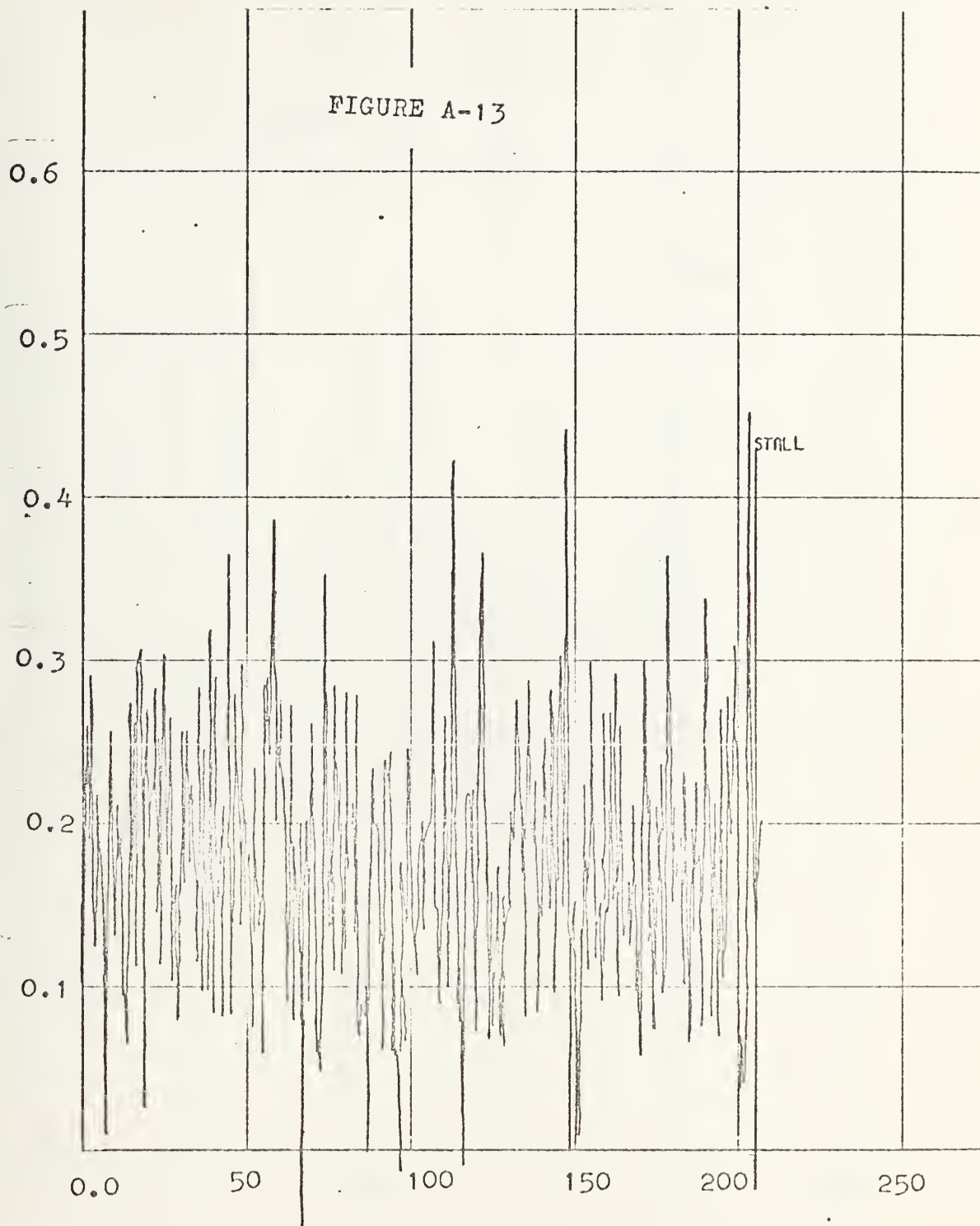
Downs Index

case four

index vs time in millisecc

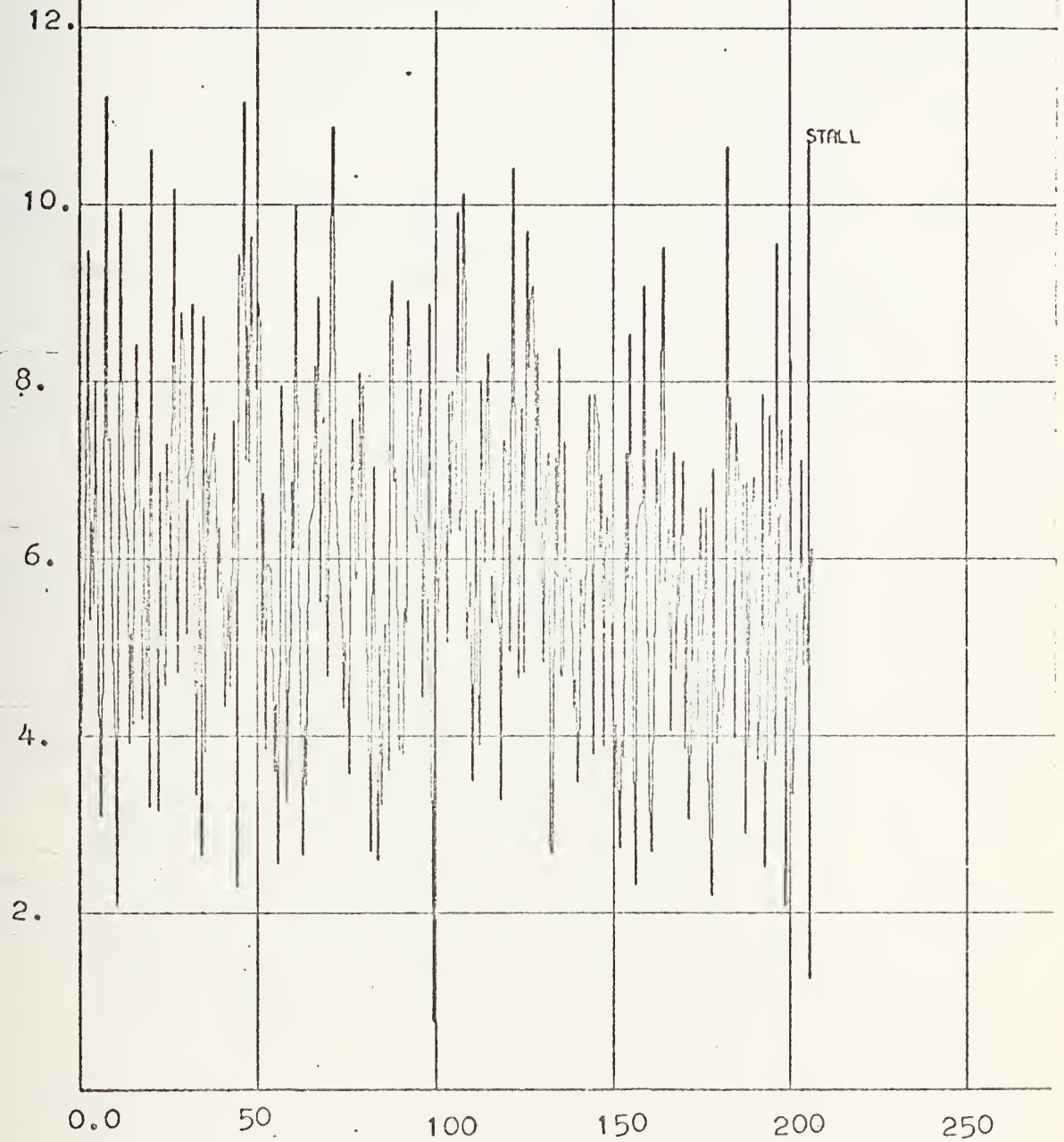


Pratt and Whitney Index
case four
index vs time in millisecc



Shoemaker Index
case five
index vs time in millisec

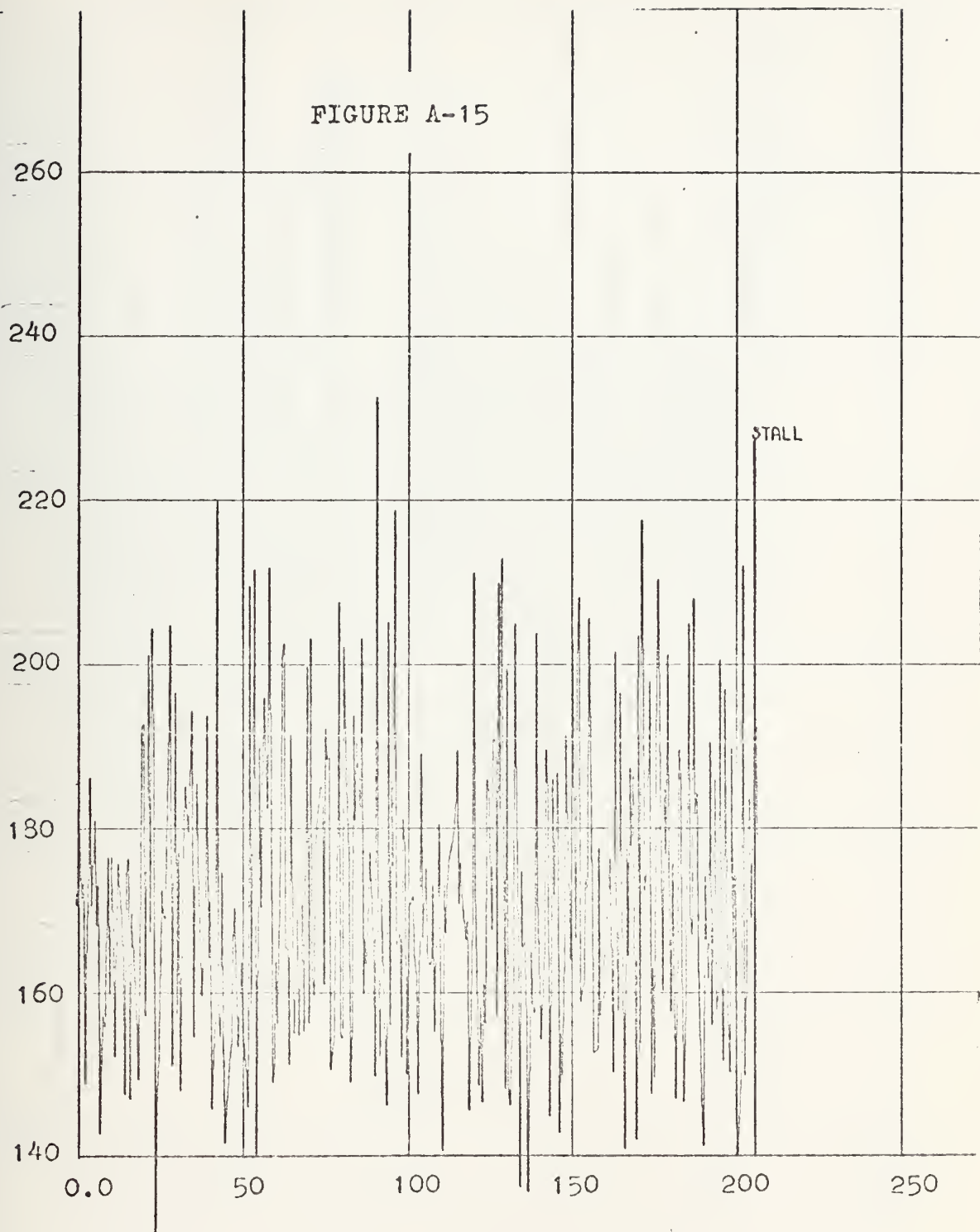
FIGURE A-14



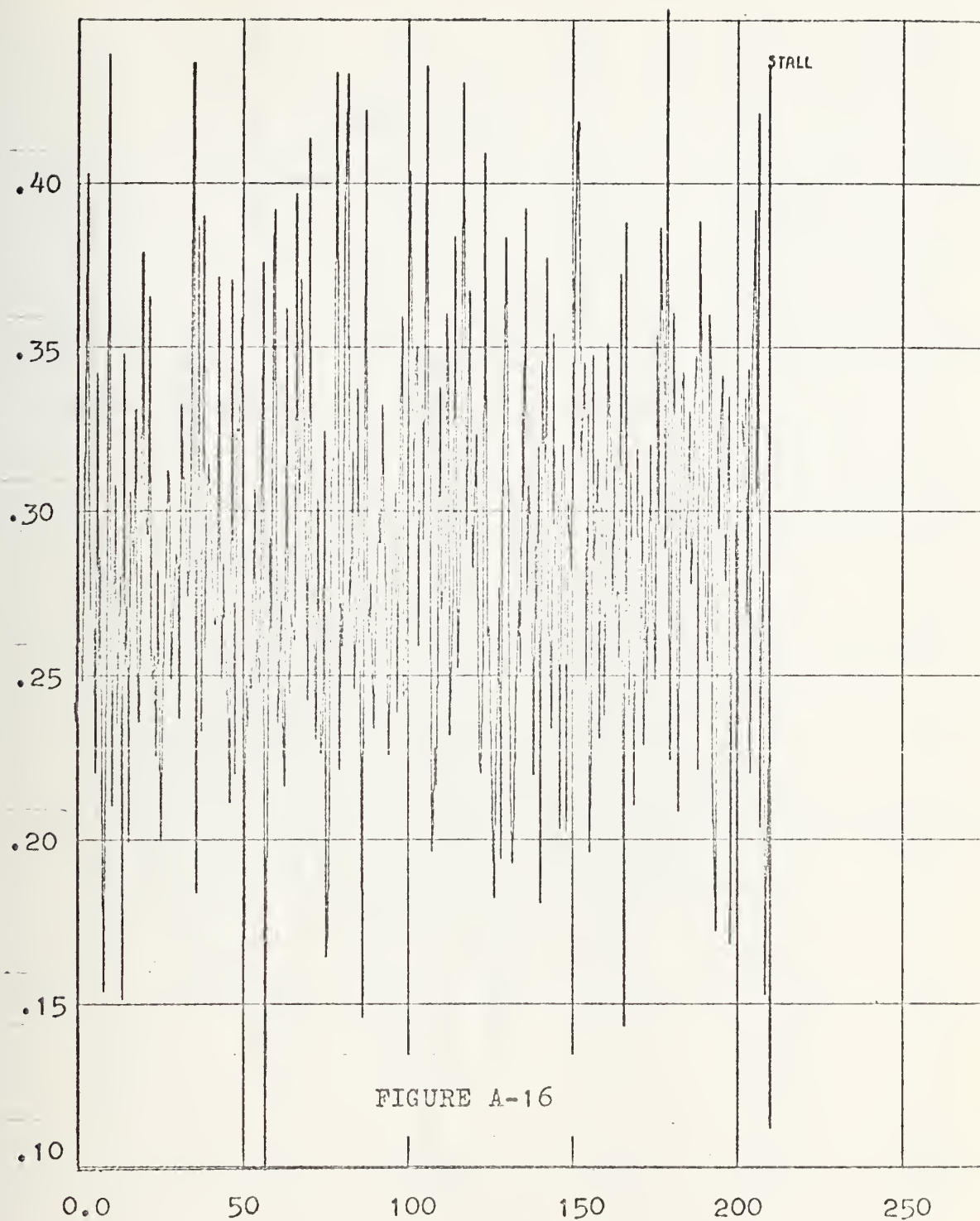
Downs Index

case five

index vs time in millisecc

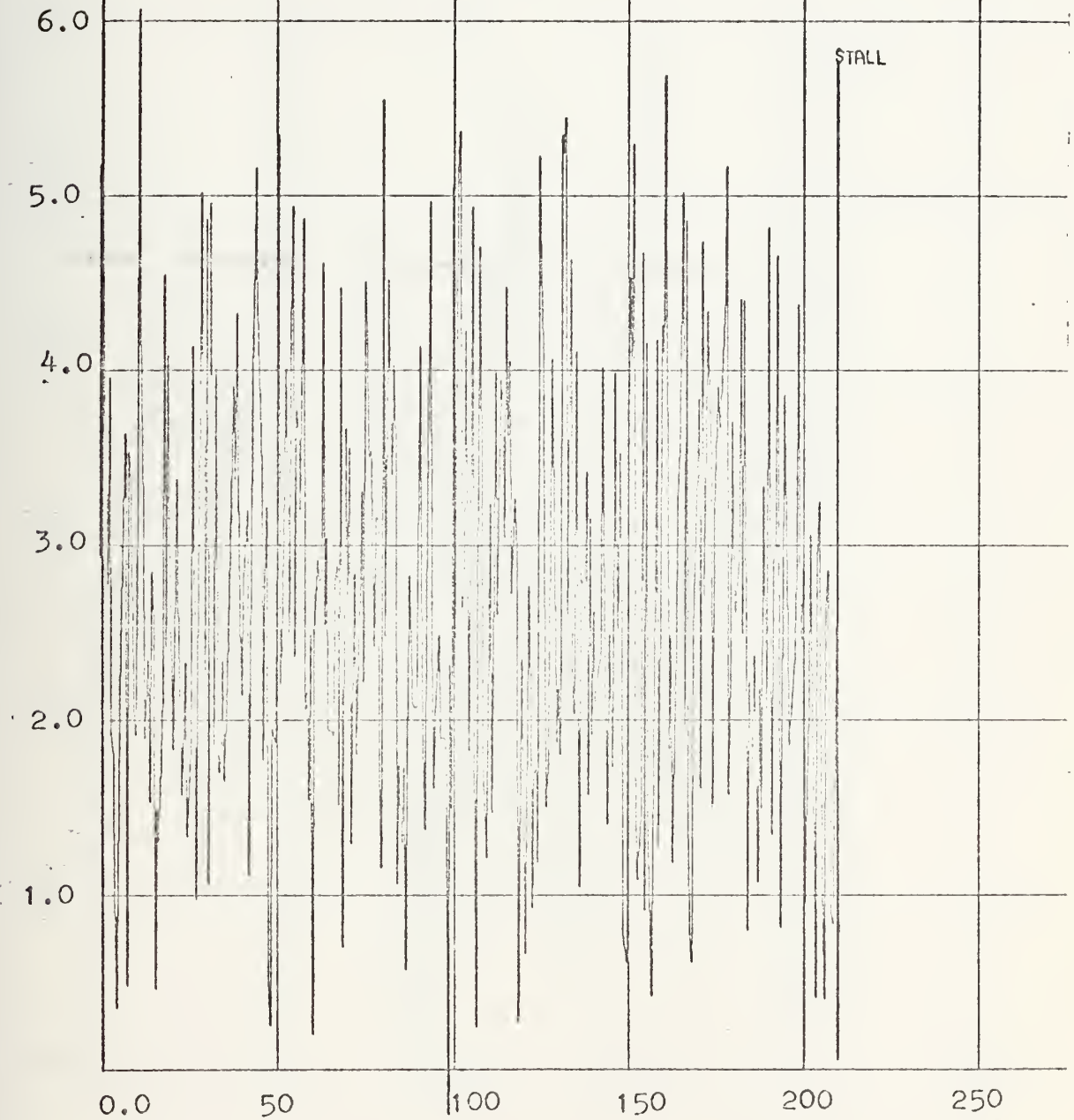


Pratt and Whitney Index
case five
index vs time in millisecc



Shoemaker Index
case six
index vs time in millisec

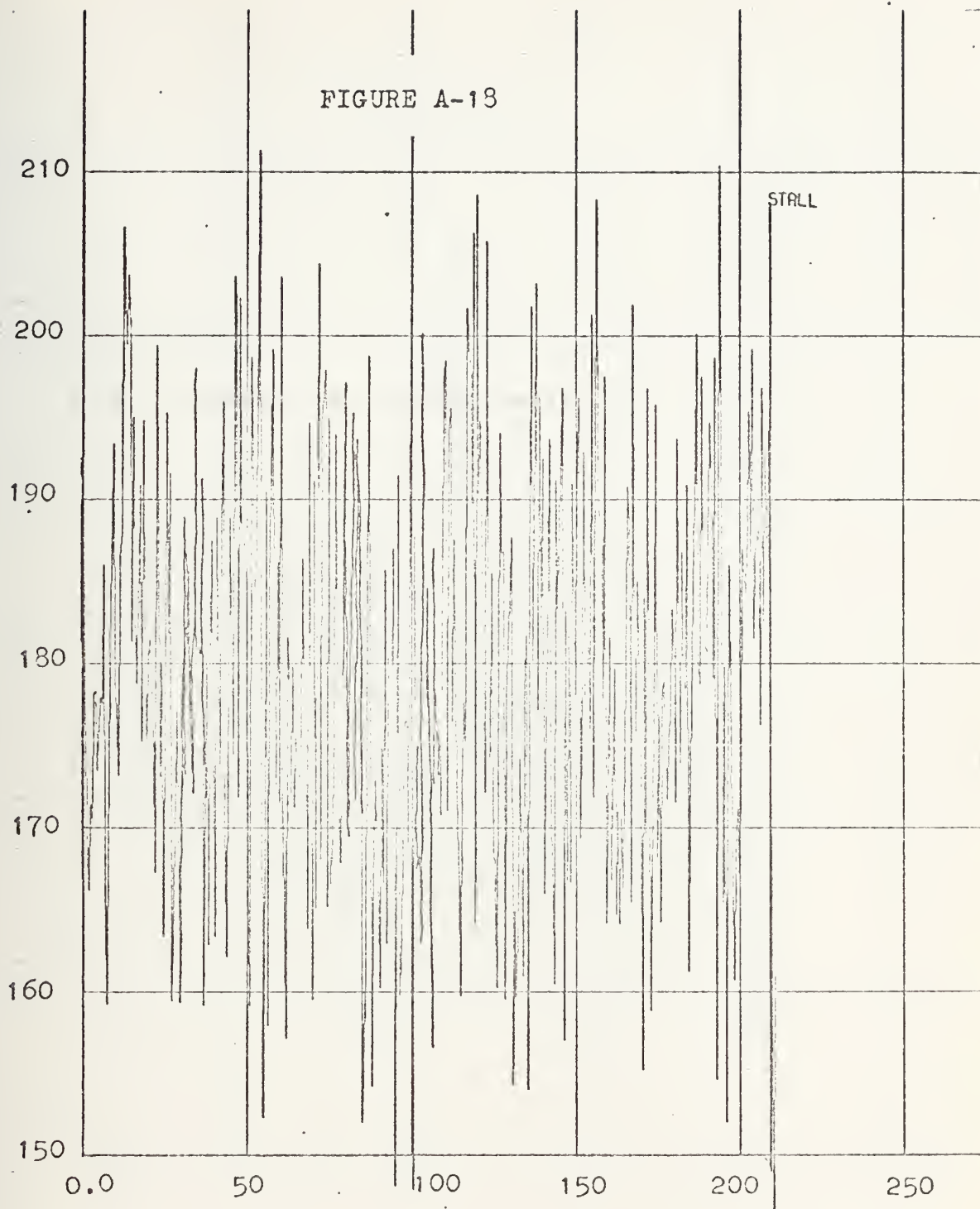
FIGURE A-17



Downs Index

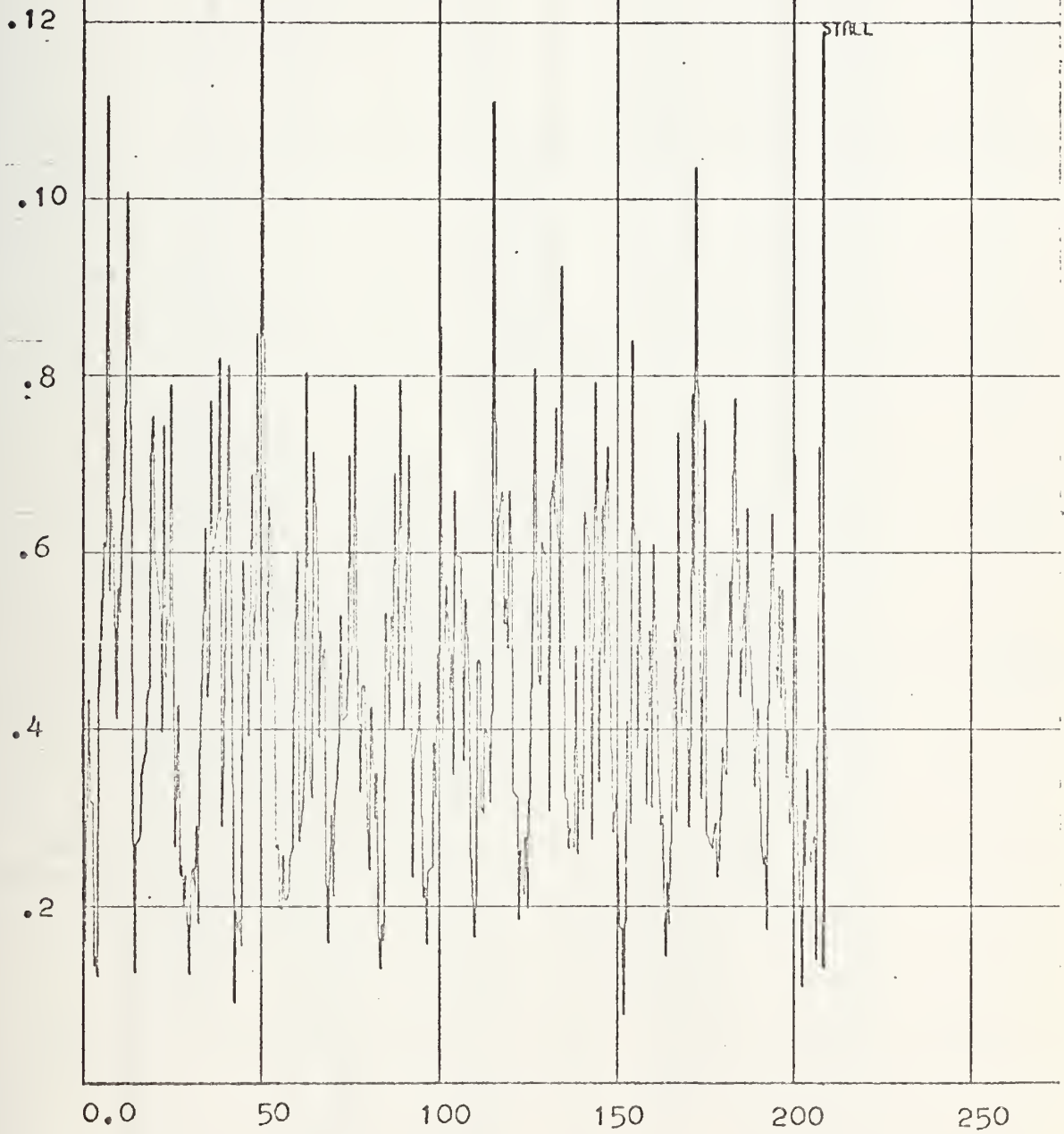
case six

index vs time in millisec



Pratt and Whitney Index
case six
index vs time in millisec

FIGURE A-19

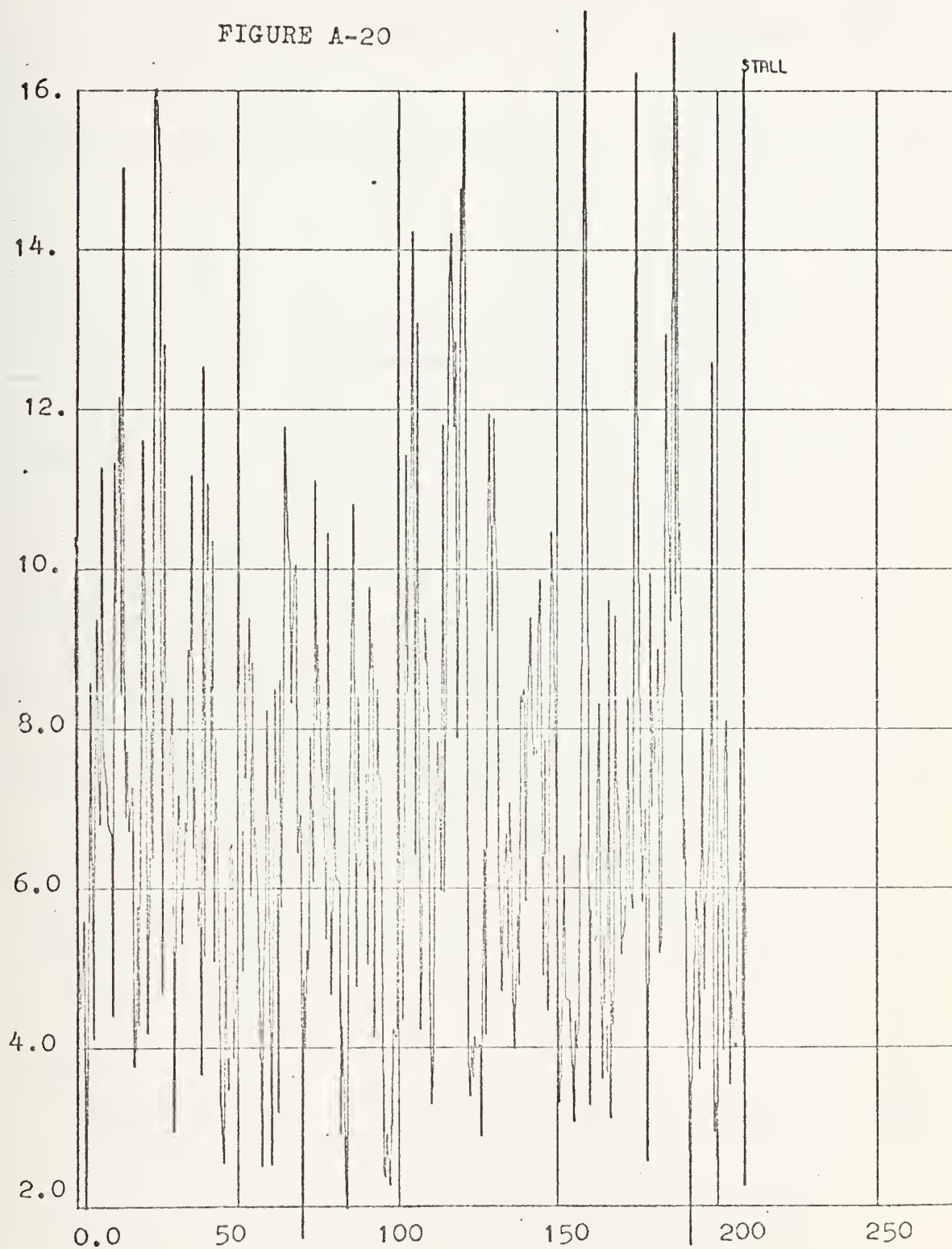


Shoemaker Index

case seven

index vs time in millisecc

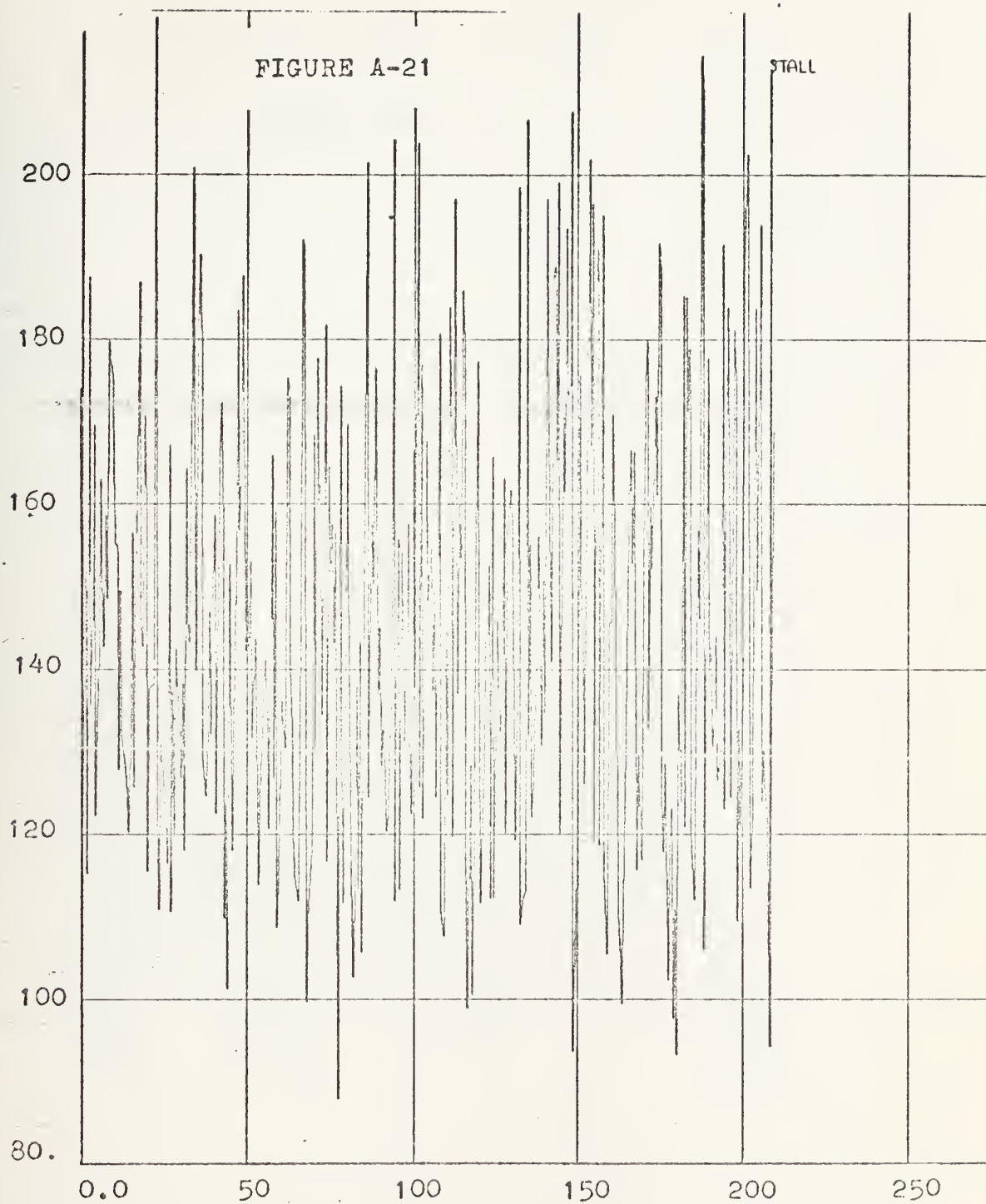
FIGURE A-20



Downs Index

case seven

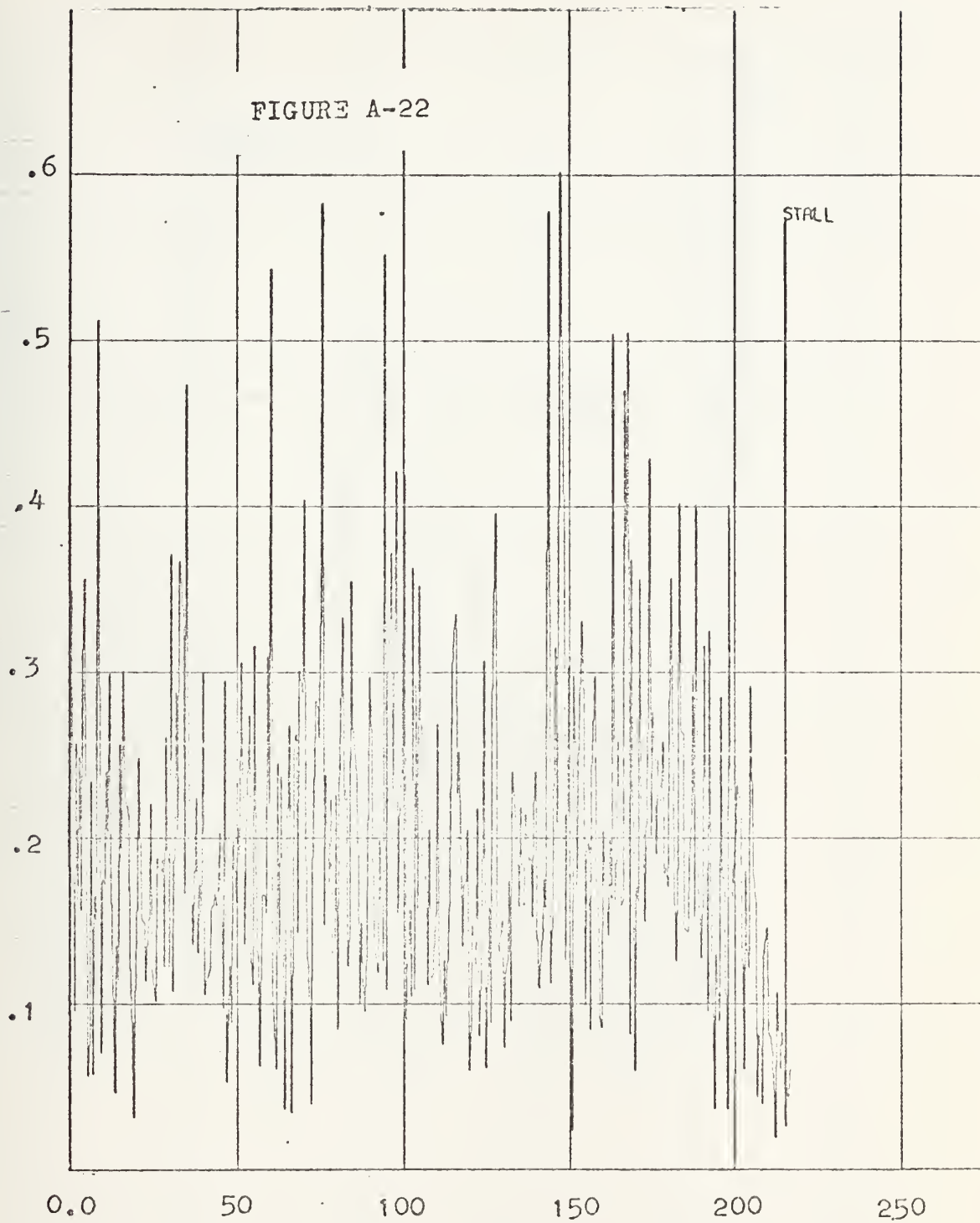
index vs time in millisec



Pratt and Whitney Index

case seven

index vs time in millisecc



Shoemaker Index

case eight

index vs time in millisecc

14.

12.

10.

8.0

6.0

4.0

2.0

0.0

50

100

150

200

250

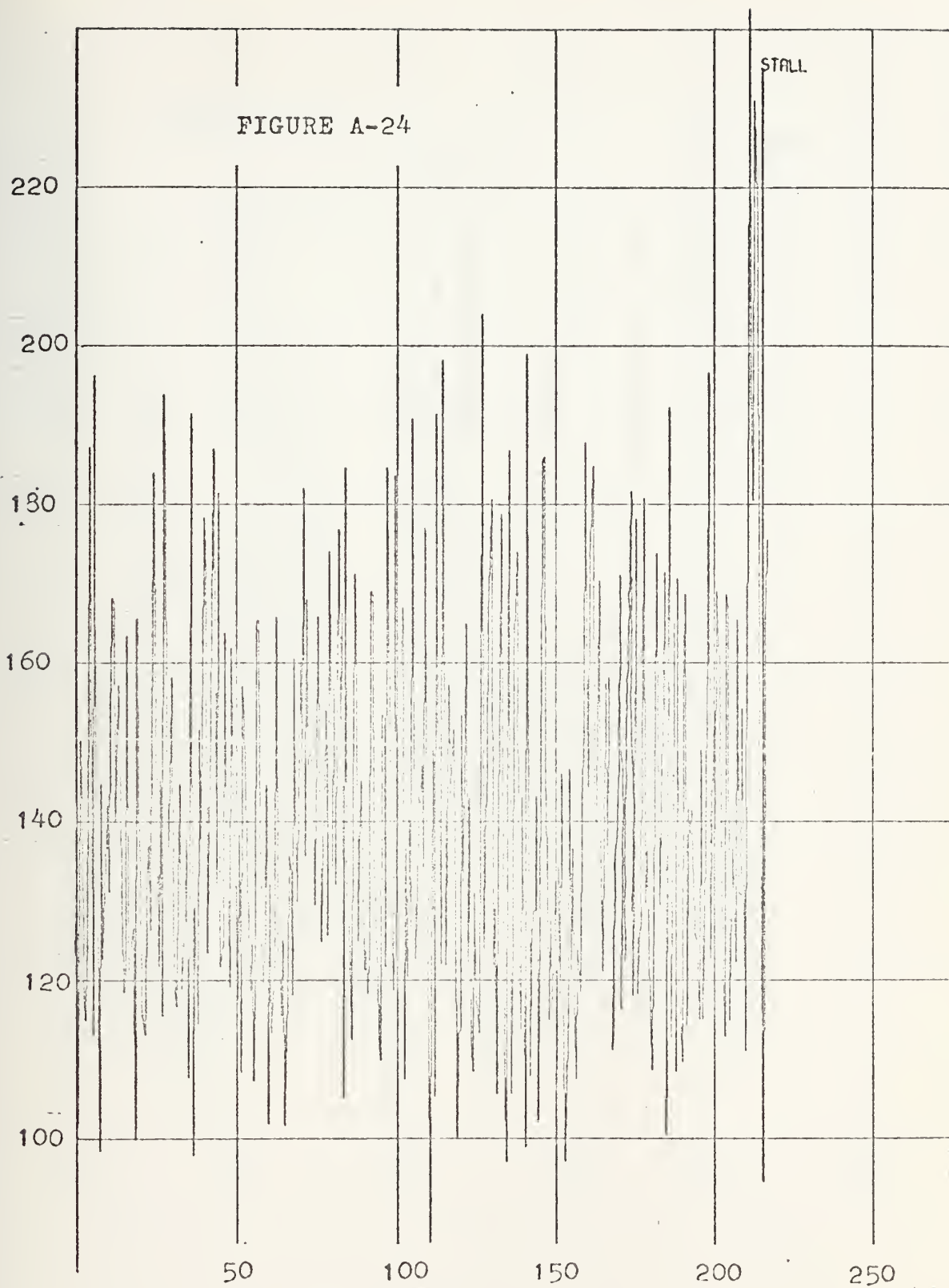
FIGURE A-23

STALL

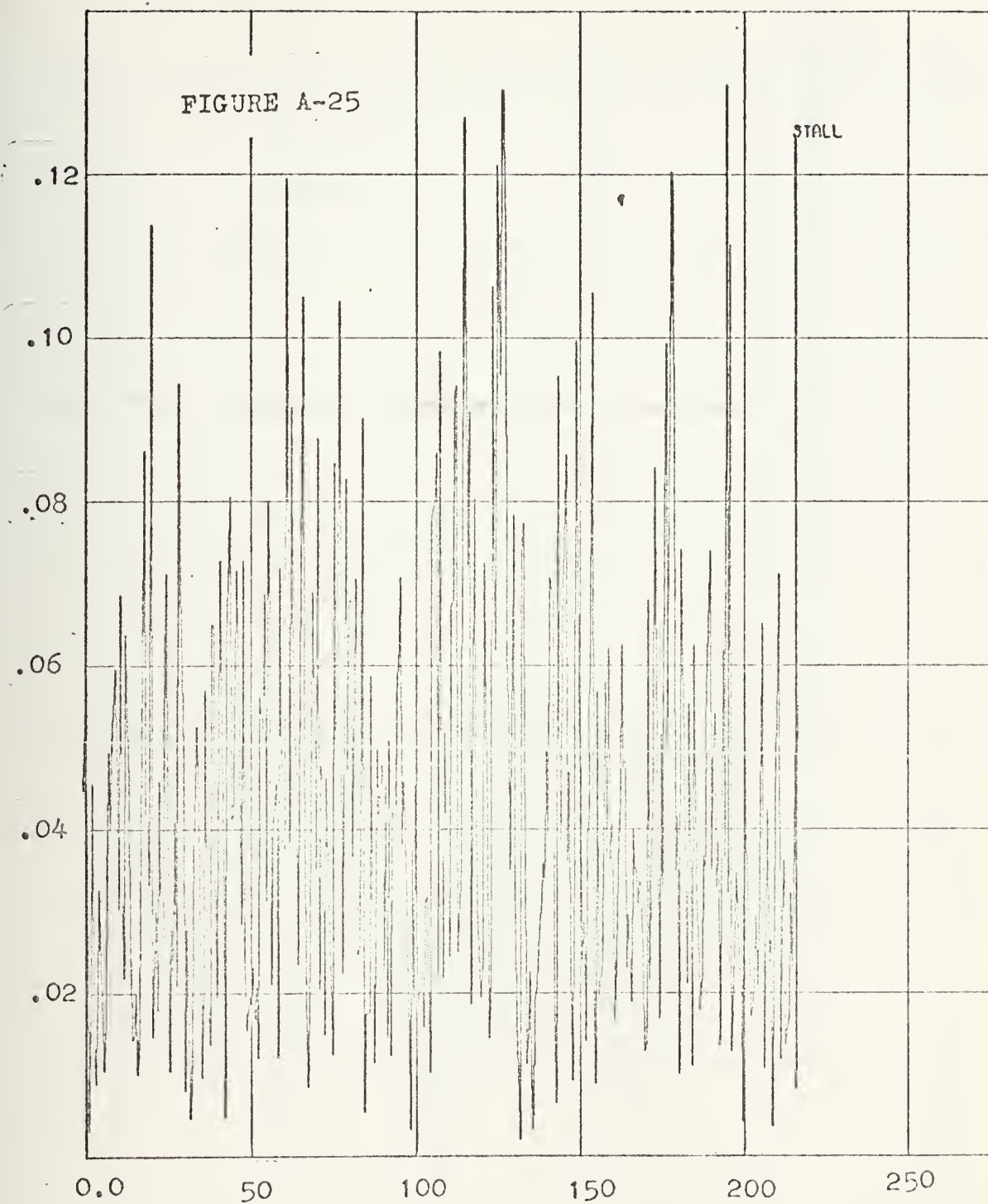
Downs Index

case eight

index vs time in millisec



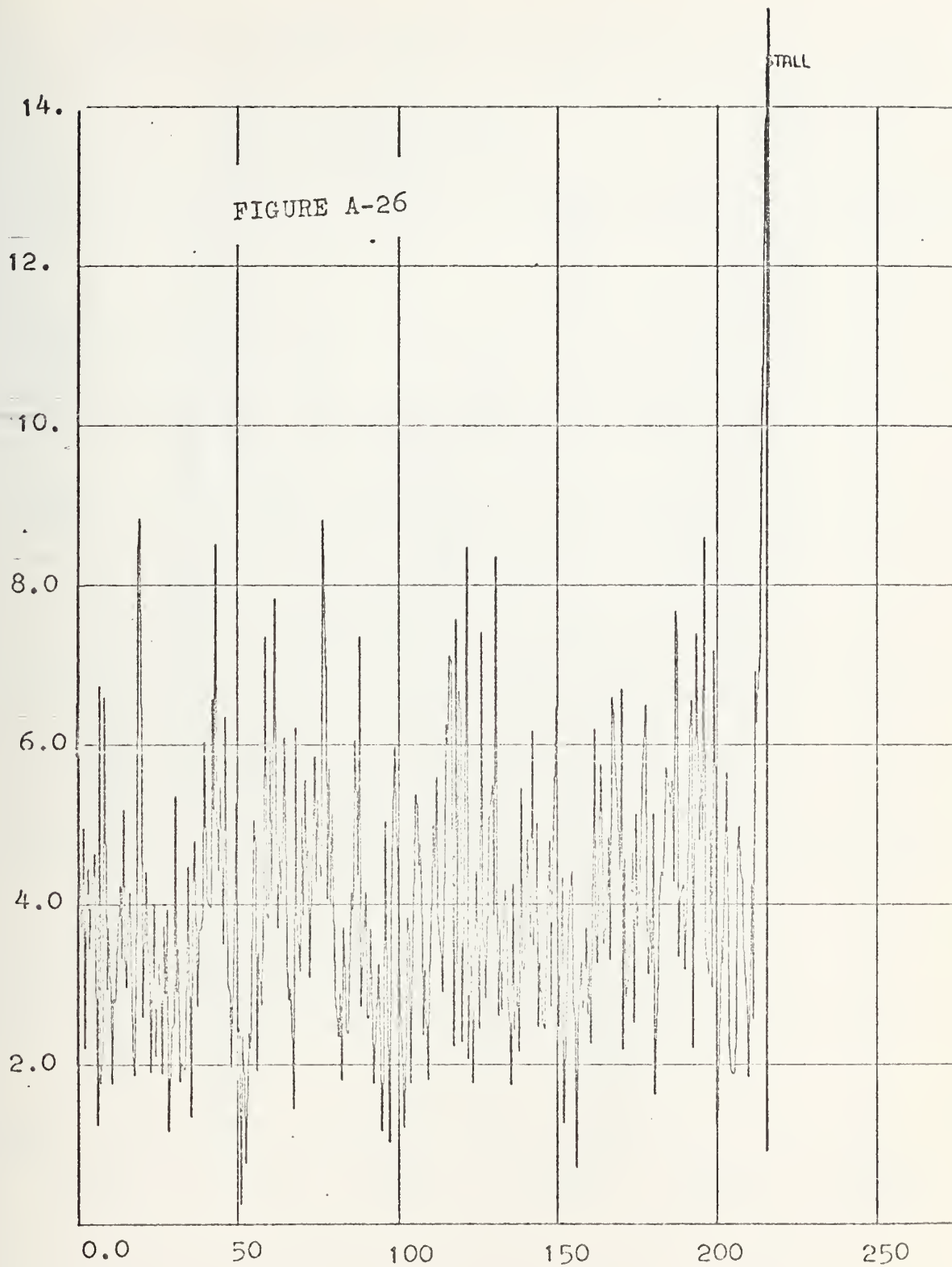
Pratt and Whitney Index
case eight
index vs time in millisec



Shoemaker Index

case nine

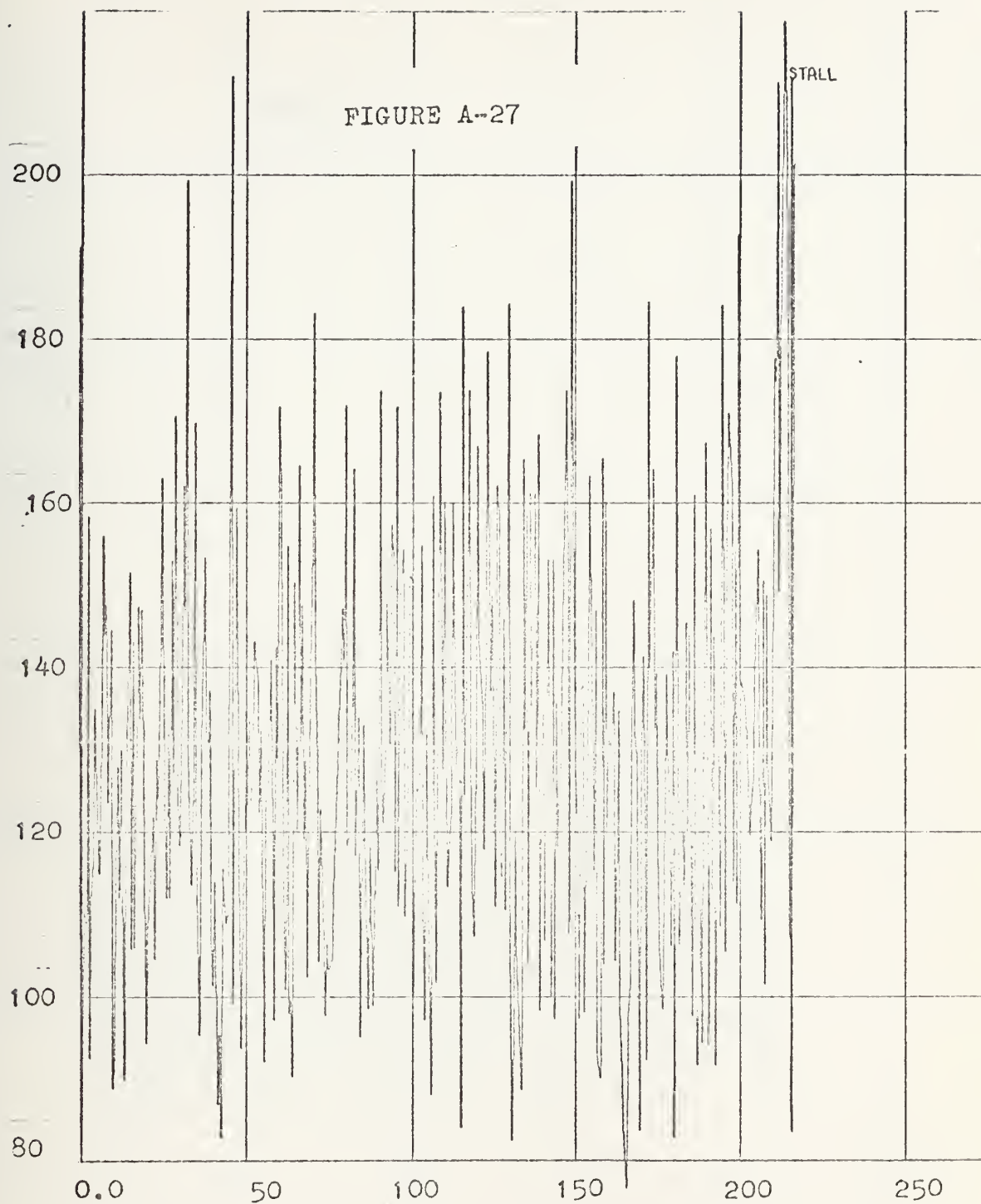
index vs time in millisec



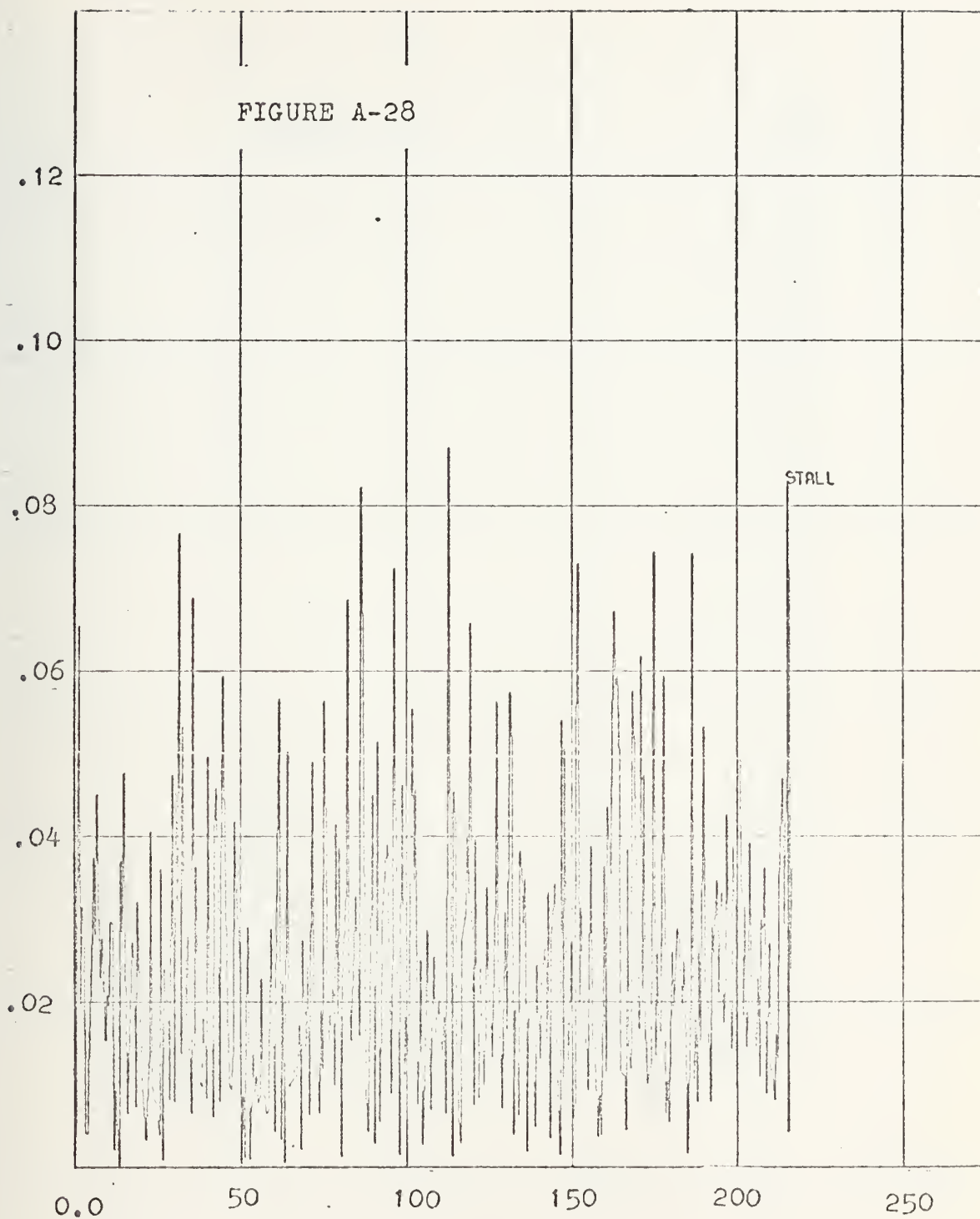
Downs Index

case nine

index vs time in millisecc



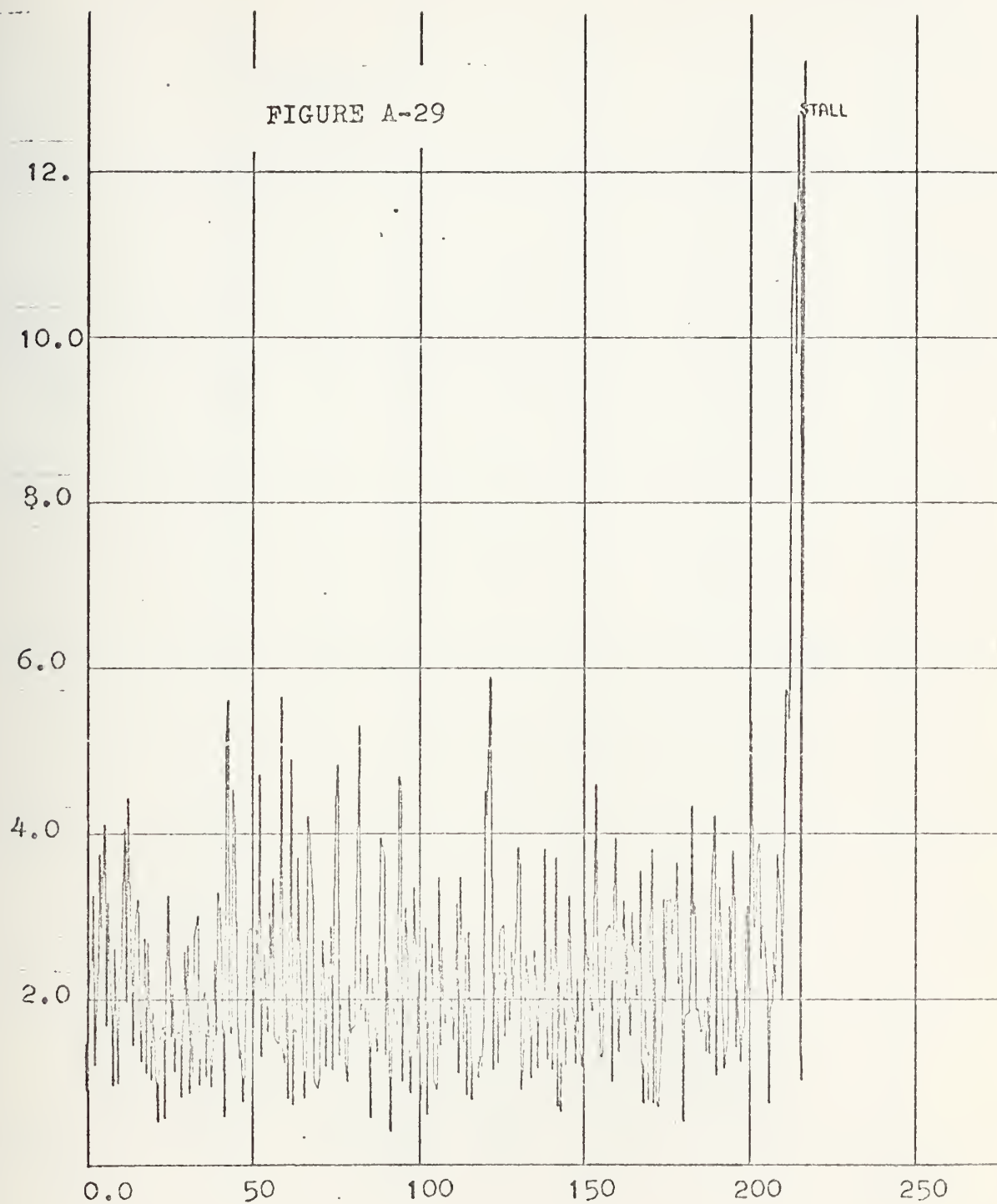
Pratt and Whitney Index
case nine
index vs time in millisecc



Shoemaker Index

case ten

index vs time in millisecc

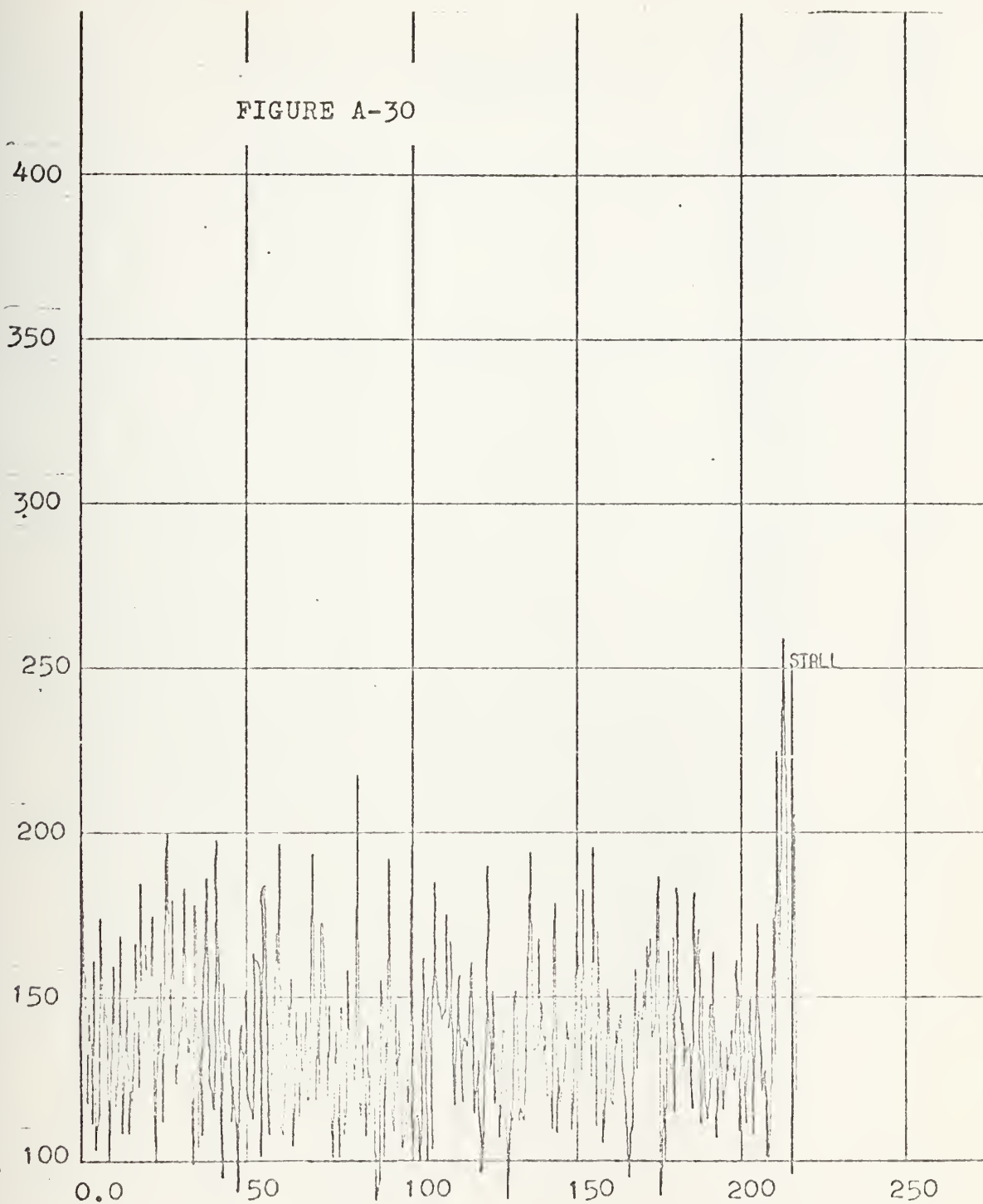


Downs Index

case ten

index vs time in millisecc

FIGURE A-30

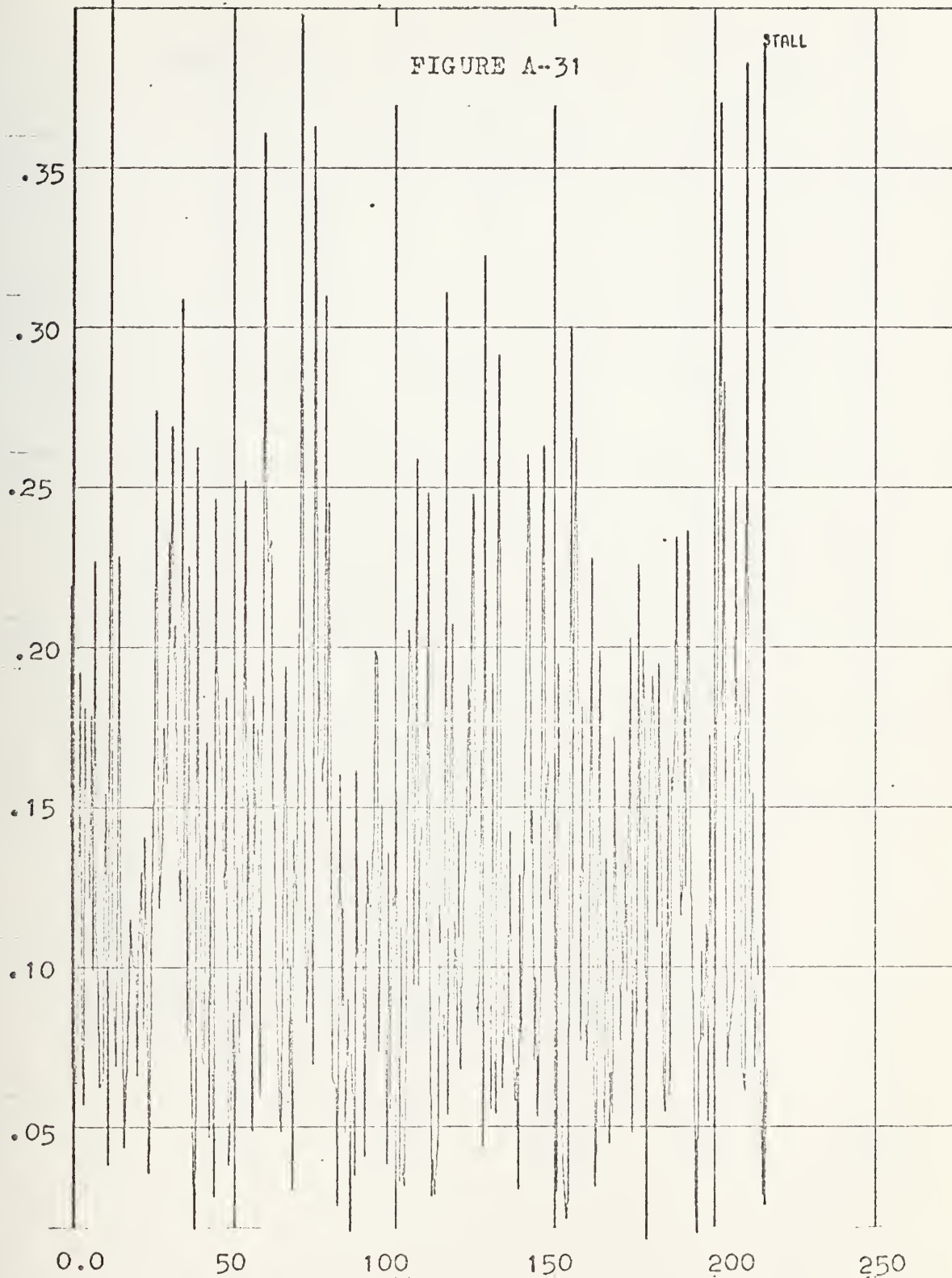


Pratt and Whitney Index

case ten

index vs time in millisecc

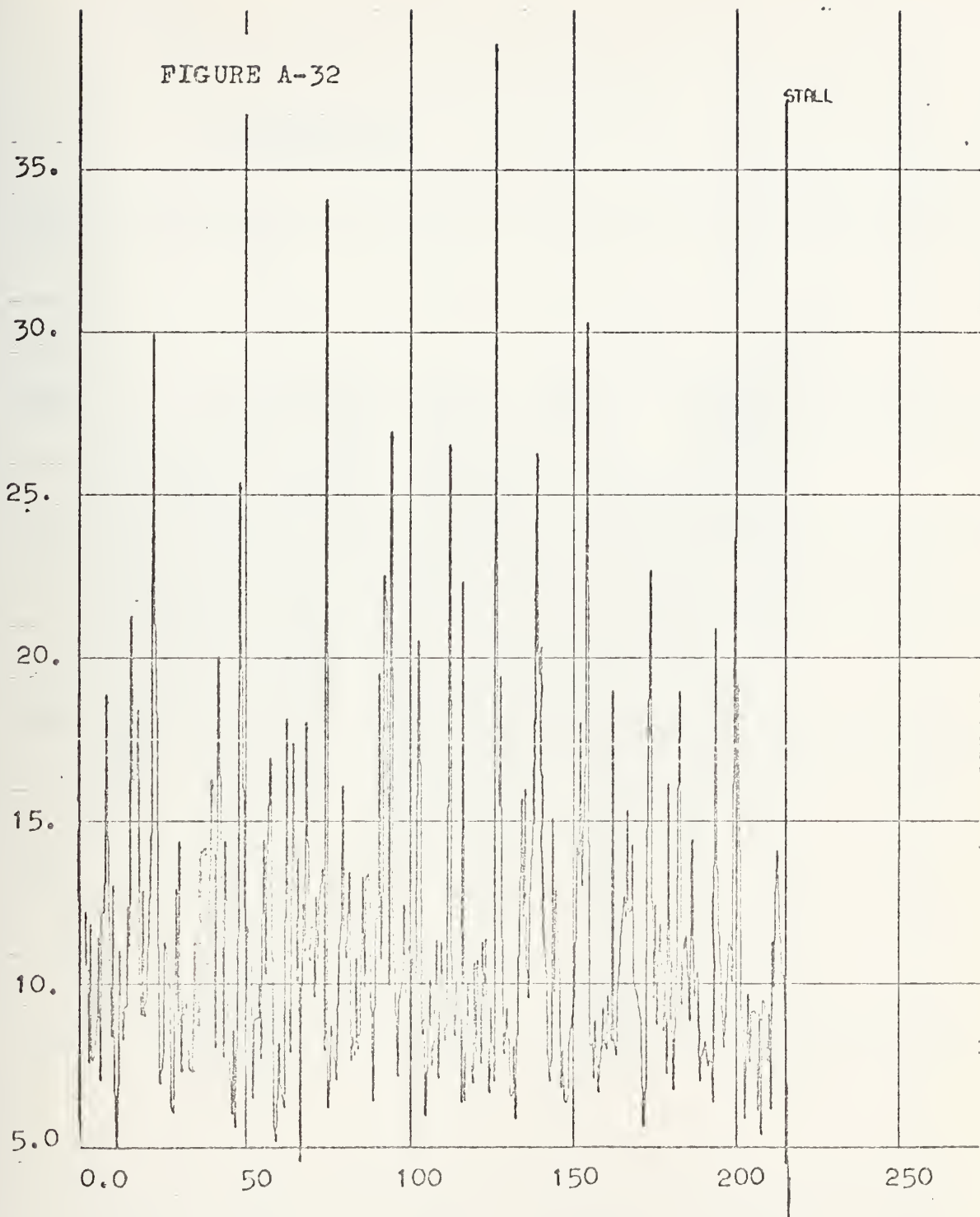
FIGURE A-31



Shoemaker Index

case eleven

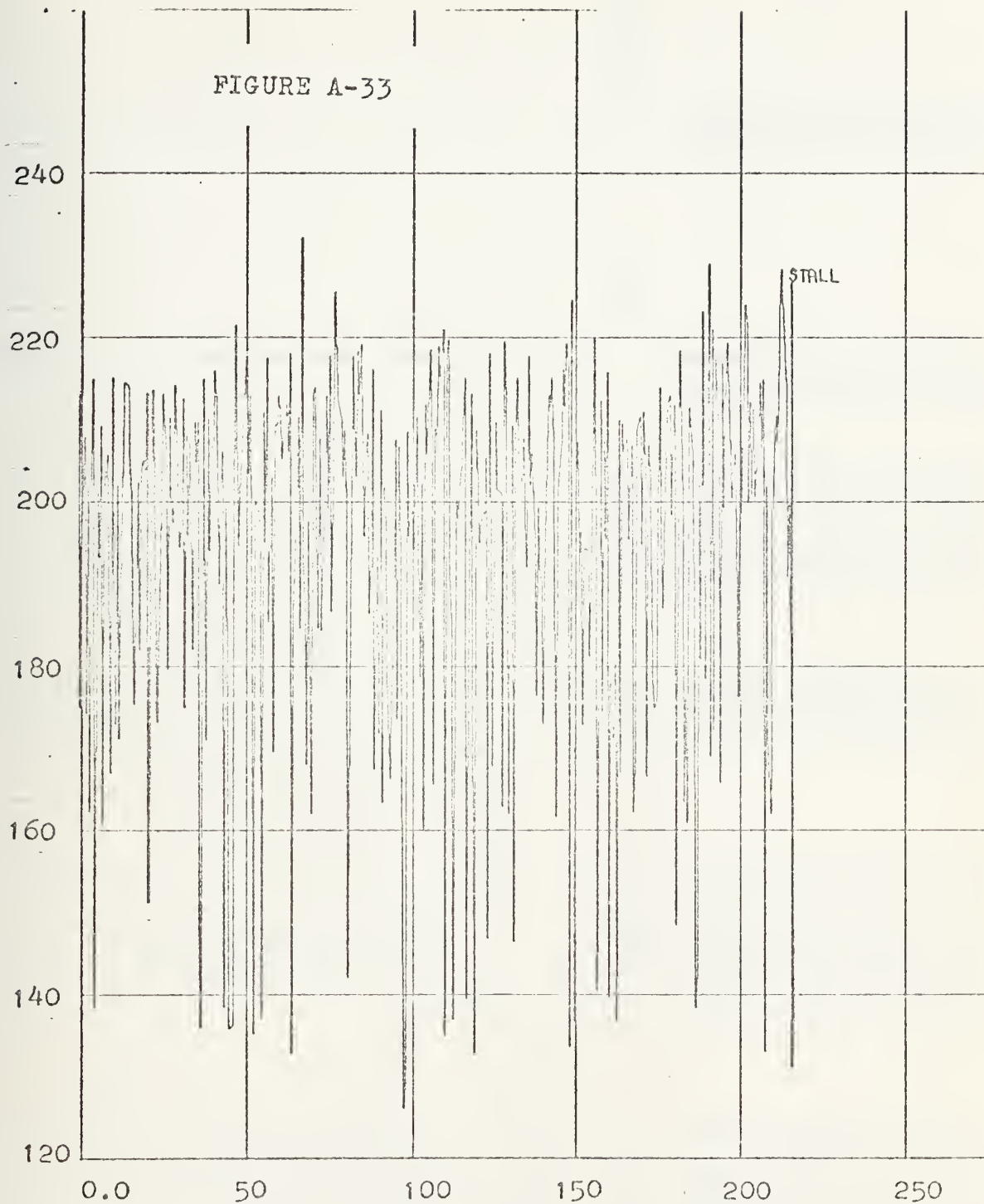
index vs time in millisecc



Downs Index

case eleven

index vs time in millisecc



Pratt and Whitney Index
case eleven
index vs time in millisec

SHUMAKER INDEX CASE 1

```

*** STALL WARNING ***      TIME IS 122.625
*** STALL WARNING ***      TIME IS 123.250
*** STALL WARNING ***      TIME IS 123.875
*** STALL WARNING ***      TIME IS 180.125
*** STALL WARNING ***      TIME IS 180.750
*** STALL WARNING ***      TIME IS 181.375
STALL OCCURRED AT TIME 202.40

```

False Warning

Stall Prediction

CASE NUMBER 1
 AVERAGE STATIC PRESSURE IS 1328.400

TAPE WAS READ 52 TIMES

N	DFACT(N)	FACT(N)	TIME	PTAVE	MEAN	STD-DEV
1	0.123555E	0.123555E	0.1250	1627.196	0.0	0.0
2	0.13216E	0.13216E	0.1250	1552.030	0.0	0.0
3	0.14304E	0.14304E	0.1300	1538.981	0.0	0.0
4	0.12172E	0.12172E	0.2250	15584.724	0.0	0.0
5	0.12167E	0.12167E	0.2250	1578.427	0.0	0.0
6	0.12919E	0.12919E	0.2875	1578.197	0.0	0.0
7	0.149221E	0.149221E	0.4175	1518.234	0.0	0.0
8	0.168846E	0.168846E	0.5375	1577.415	0.0	0.0
9	0.152506E	0.152506E	0.6000	1577.816	0.0	0.0
10	0.174898E	0.174898E	0.6625	1607.050	0.0	0.0
11	0.15914E	0.15914E	0.7375	1589.720	0.0	0.0
12	0.14295E	0.14295E	0.8125	1578.567	0.0	0.0
13	0.14295E	0.14295E				
14	0.14295E	0.14295E				
15	0.14295E	0.14295E				

4461E 00

8906E 00

[illegible][illegible][illegible][illegible]

1433E 00

00 35800

91	1	2	3	4	5	6	7	8	9	10	11	12	13	14	15	16	17	18	19	20	21	22	23	24	25	26	27	28	29	30	31	32	33	34	35	36	37	38	39	40	41	42	43	44	45	46	47	48	49	50
91	1	2	3	4	5	6	7	8	9	10	11	12	13	14	15	16	17	18	19	20	21	22	23	24	25	26	27	28	29	30	31	32	33	34	35	36	37	38	39	40	41	42	43	44	45	46	47	48	49	50
92	1	2	3	4	5	6	7	8	9	10	11	12	13	14	15	16	17	18	19	20	21	22	23	24	25	26	27	28	29	30	31	32	33	34	35	36	37	38	39	40	41	42	43	44	45	46	47	48	49	50
93	1	2	3	4	5	6	7	8	9	10	11	12	13	14	15	16	17	18	19	20	21	22	23	24	25	26	27	28	29	30	31	32	33	34	35	36	37	38	39	40	41	42	43	44	45	46	47	48	49	50
94	1	2	3	4	5	6	7	8	9	10	11	12	13	14	15	16	17	18	19	20	21	22	23	24	25	26	27	28	29	30	31	32	33	34	35	36	37	38	39	40	41	42	43	44	45	46	47	48	49	50
95	1	2	3	4	5	6	7	8	9	10	11	12	13	14	15	16	17	18	19	20	21	22	23	24	25	26	27	28	29	30	31	32	33	34	35	36	37	38	39	40	41	42	43	44	45	46	47	48	49	50
96	1	2	3	4	5	6	7	8	9	10	11	12	13	14	15	16	17	18	19	20	21	22	23	24	25	26	27	28	29	30	31	32	33	34	35	36	37	38	39	40	41	42	43	44	45	46	47	48	49	50
97	1	2	3	4	5	6	7	8	9	10	11	12	13	14	15	16	17	18	19	20	21	22	23	24	25	26	27	28	29	30	31	32	33	34	35	36	37	38	39	40	41	42	43	44	45	46	47	48	49	50
98	1	2	3	4	5	6	7	8	9	10	11	12	13	14	15	16	17	18	19	20	21	22	23	24	25	26	27	28	29	30	31	32	33	34	35	36	37	38	39	40	41	42	43	44	45	46	47	48	49	50
99	1	2	3	4	5	6	7	8	9	10	11	12	13	14	15	16	17	18	19	20	21	22	23	24	25	26	27	28	29	30	31	32	33	34	35	36	37	38	39	40	41	42	43	44	45	46	47	48	49	50
100	1	2	3	4	5	6	7	8	9	10	11	12	13	14	15	16	17	18	19	20	21	22	23	24	25	26	27	28	29	30	31	32	33	34	35	36	37	38	39	40	41	42	43	44	45	46	47	48	49	50
101	1	2	3	4	5	6	7	8	9	10	11	12	13	14	15	16	17	18	19	20	21	22	23	24	2																									

[illegible]

75

3820E 00

7075E 00

2571890
22590
226123
22645
22677
2268
22711
22723
22745
22777
22790
22834
22845
22878
22890
22934
22945
22967
22989
22990
23000

0:0
0:0
0:0
0:0
0:0
0:0

0:0
0:0
0:0
0:0
0:0
0:0

1574.448
1585.029
1503.822
1556.801
1578.629
1563.658
1579.467

200.750
201.375
202.000
202.625
203.250
203.875
204.125
FOR NEXT CASE

00
00
00
01
01
00
01
TO REPOSITION

0.85671E
0.51978E
0.54192E
0.14755E
0.11566E
0.14203E
0.13235E
TO REPOSITION

0.58754E
0.66019E
0.66280E
0.84573E
0.10580E
0.11580E
0.11073E
READ 12 TIMES

TAPE WAS
352
353
354
355
356
357
358

[illegible][illegible][illegible]

VANN0001
VANN0002
VANN0003
VANN0004
VANN0005
VANN0006
VANN0007
VANN0008
VANN0009
VANN0010
VANN0011
VANN0012
VANN0013
VANN0014
VANN0015
VANN0016
VANN0017
VANN0018
VANN0019
VANN0020
VANN0021
VANN0022
VANN0023

VANN0024
VANN0025
VANN0026
VANN0027
VANN0028
VANN0029
VANN0030
VANN0031
VANN0032
VANN0033
VANN0034
VANN0035
VANN0036
VANN0037

```
DATA PI/3.14157/  
DATA THETA/0.,20.,40.,60.,80.,100.,120.,140.,160.,180.,  
A200.,220.,240.,260.,280.,300.,320.,340.,360./  
DATA TITLE4//  
DATA TITLE6//STAL//  
B=72.0*10.0/3094.0  
CAL=4096  
DO 17 N=1,9  
  THETA(N)=THETA(N)*PI/180.0  
17 DO 75 N=1,NAIX  
  ANGLE(N)=THETA(N)  
  THETA(N)=THETA(N)*PI/180.0  
75 CONTINUE
```

CCCCC THE FOLLOWING DO LOOP POSITIONS THE TAPE TO THE DESIRED
STARTING POINT. USE FORMULA NRUNS=(3+FIRST CASE NUMBER)*64

VANN0036
VANN0037
VANN0038
VANN0039

```
NRUNS=4*64  
DO 27 N=1,NRUNS  
  READ(4,105,END=1020,ERR=1021) TAPE  
27 CONTINUE
```

THE FOLLOWING CARD, 1008 CONTINUE, IS A SWITCHING POINT TO BE ENTERED
WHEN A NEW CASE IS TO BE CONSIDERED.

VANN0040
VANN0041
VANN0042
VANN0043
VANN0045
VANN0046
VANN0047
VANN0048
VANN0049
VANN0050
VANN0051

```
1008 CONTINUE  
  READ(5,1010,END=1007) NRUN,NSTOP,STALL,PSTATIC  
  READ(5,1003) TTILES  
  WRITE(6,1071) (TTILES(I),I=1,6)  
  ITIMES=0  
  JTIMES=1  
  JMAP=-1  
  STALL2(1)=1.E20  
  STALL2(2)=0.0  
  NFAC=1
```

THE VALUES OF STATIC PRESSURE AT EACH OF THE PROBES
ARE READ IN HERE

VANN0052
VANN0053

```
DO 1 N=2,7  
  READ(5,103)(PO(N,J),J=1,7)
```

THE VALUES OF THE PRESSURES AT AN ANGLE OF 360 ARE
SET EQUAL TO THE PRESSURES AT AN ANGLE OF 0
IN ORDER TO ASSURE THAT THE INTERPOLATION SCHEME
WILL BE SMOOTH

CCCCC

C

```

50 J=1.7
  PC(9,J)=PO(3,J)
  PC(1,J)=PO(7,J)
50 PC(8,J)=PO(2,J)
  PSUM=0.0 DOO
  DC 2 N=2,7
  DC 2 J=2,5
  PSUM=PSUM+PO(N,J)
  PAVE=PSUM/30.0D'00
  DC 65 I=1,9
  DC 65 J=1,7
  PC(I,J)=PO(I,J)/PAVE
65 CONTINUE

```

CCCCCC STATEMENT 100 US A SWITCHING POINT THAT CAN BE RETURNED TO
IN ORDER TO CALCULATE VALUES OF VORTICITY FOR THE SAME
STATIC PRESSURES BUT DIFFERENT DYNAMIC PRESSURES
USED IN THE CALCULATION OF VORTICITY

```

100 CONTINUE
  NMAP=NMAP+2
  READ(4,105,END=1024,ERR=1025) TAPED
  ITIMES=ITIMES+1
  DC 600 N=1,32
  JUST=(N-1)*30+1
  DC 600 J=JUST, JEST
  KLAP=J-JUST+1
  INTRIM(N,KLAP)=TAPED(J)
  CONTINUE
600 NCASE=1
  DC 605 N=2,7
  JUST=(N-2)*5+1
  DC 605 J=JUST, JEST
  DC 605 J=JUST+2
  KLAP=J-JUST+1
  KCOUNT(N,KLAP)=INTRIM(NCASE,J)
605 CONTINUE
  READ FOLLOWING CARDS, TO 500 WRITE ECHO CHECK THE VALUES OF TOTAL PRESSURE  
THAT FOLLOW THE TAPE. DELETE IF NOT DESIRED. INSERT AFTER 605 CONTINUE
  CCCC
  WRITE(6,213) NRUN,NMAP
  WRITE(6,209)
  DC 500 I=2,7
  WRITE(6,210)(MCOUNT(I,J),J=2,6)
  NCASE=NCASE+5
  ICAASE=NMAP
500 CONTINUE

```

VANN0341
VANN0054
VANN0055
VANN0056
VANN0057
VANN0058
VANN0059
VANN0060
VANN0061
VANN0062
VANN0063
VANN0064
VANN0065

VANN0066
VANN0067
VANN0068
VANN0069
VANN0070
VANN0071
VANN0072
VANN0073
VANN0074
VANN0075
VANN0076
VANN0077
VANN0078
VANN0079
VANN0080
VANN0081
VANN0082
VANN0083
VANN0084
VANN0085
VANN0086
VANN0087
VANN0088
VANN0089
VANN0090

[illegible]

USE ONE OF THE FOLLOWING THREE INDICES

UUU

C

START SHUMAKER INDEX

CALL SPLIN2(THETA,RP,VORT,NAIX,NR)

FAC(NFACT)=0.

DO 799 NCOMP=i,30

XT=(NCOMP*12.0)*PI/180.0

SPFACT=0.

DO 853 JFACT=1,4

XY=RFAC(JFACT)

PFAC=F2(XT,XY)

IF (PFAC*LT*0.) PFAC=0.

SPFACT=SPFACT+PFAC

CONTINUE

DO 854 JFACT=5,8

XY=RFAC(JFACT)

FACM=F2(XT,XY)

IF (FACM*GT*0.) FACM=0.

SPFACT=SPFACT+FACM

CONTINUE

FAC(NFACT)=FAC(NFACT)+SPFACT-SFACTM

CONTINUE

FAC(NFACT)=FAC(NFACT)/(8.0*30.0)

END SHUMAKER INDEX

START DOWNS INDEX

FIRST WORK ON (PTAVE-PT)/PTAVW COMPONENT

DO 1050 I=1,30

XT=FLCAT(I)*12.0*PI/180.0

PFAC=0.0

DO 1051 J=1,7

XY=.25*FLOAT(J)*.1

PFAC=PFAC+1.0-F2(XT,XY)

CONTINUE

RADIAL(I)=PFAC

DO 1052 I=1,4

J=I+30

RADIAL(J)=RADIAL(I)

CONTINUE

DO 1053 I=1,30

PFAC=0.0

L=I+4

DO 1054 J=1,L

PFAC=PFAC+RADIAL(J)

CONTINUE

VANN0136
VANN0137
VANN0138
VANN0139
VANN0140
VANN0141
VANN0142
VANN0143
VANN0144
VANN0145
VANN0146
VANN0147
VANN0148
VANN0149
VANN0150
VANN0151
VANN0152
VANN0153
VANN0154
VANN0155
VANN0156

VANN0157
VANN0158
VANN0159
VANN0160
VANN0161
VANN0162
VANN0163
VANN0164
VANN0165
VANN0166
VANN0167
VANN0168
VANN0169
VANN0170
VANN0171
VANN0172
VANN0173
VANN0174


```

1053 CIRCUM(I)=PFAC
1054 CONTINUE
C
C
C      NOW WORK ON RADIAL VORTEX COMPONENT
CALL SPLIN2(THETA,RP,VORTRA,NAIX,NR)
DC 1055 I=1,30
XT=FLOAT(I)*12.0*PI/180.0
PFACI=0.0
DO 1056 J=1,7
XY=.25+FLOAT(J)*.1
PFACI=PFACI+PF2(XT,XY)
CONTINUE
1056 RADIAL(I)=PFACI
CONTINUE
1057 DO 1057 I=1,4
J=I+30
RADIAL(J)=RADIAL(I)
CONTINUE
1057 DC 1058 I=1,30
PFACI=0.0
L=I+4
DC 1059 J=I,L
PFACI=PFACI+RADIAL(J)
CONTINUE
1059 CIRCUM(I+30)=PFACI
CONTINUE
1058
C
C
C      NOW ADD RADIAL AND PRESSURE COMPONENTS, SEARCH FOR LARGEST
HOLD1=0.0
DO 1060 I=1,30
J=I+30
PFACI=CIRCUM(I)+CIRCUM(J)
IF(PFACI.GT.HOLD1) HOLD1=PFACI
CONTINUE
1060 PFACI(NFACI)=HOLD1
C
C
C      END DOWNS INDEX
START COMPUTATION OF PRATT & WHITNEY INDEX K(DM)
CALL SPLIN2(THETA,RP,PP,NT,NR)
KDM=0.0
HOLD6=0.0
DC 1047 N=1,5
XY=.1375+FLOAT(N)*.1625
HOLD1=0.0
HOLD2=1.E99

```

VANN0175
VANN0176

VANN0177
VANN0178
VANN0179
VANN0180
VANN0181
VANN0182
VANN0183
VANN0184
VANN0185
VANN0186
VANN0187
VANN0188
VANN0189
VANN0190
VANN0191
VANN0192
VANN0193
VANN0194
VANN0195
VANN0196
VANN0197
VANN0198

VANN0199
VANN0200
VANN0201
VANN0202
VANN0203
VANN0204
VANN0205

VANN0206
VANN0207
VANN0208
VANN0209
VANN0210
VANN0211
VANN0212


```

HCLD3=0.0
DO 1043 I=1,30
  XT={FLCAI(I)*12.0}*PI/180.0
  PTKEEP(I)=F2(XT,XY)*PTAVE
  HCLD1=HOLD1+PTKEEP(I)
  IF(PTKEEP(I).GT.HCLD3) HCLD3=PTKEEP(I)
  IF(PTKEEP(I).LT.HCLD2) HCLD2=PTKEEP(I)
  CONTINUE
HOLD1=HOLD1/30.0
DO 1044 I=1,30
  IF(PTKEEP(I).GT.HOLD1) GO TO 1045
  J=I+1
HOLD4=0.0
HOLD5=0.0
DO 1048 K=J,30
  IF(PTKEEP(K).GT.HOLD1) HOLD4=0.0
  HCLD4=HOLD4+1.0
  IF(HCLD4.GT.HOLD5) HOLD5=HOLD4
  CONTINUE
K=1,I
DO 1046 I=1,30
  IF(PTKEEP(K).GT.HOLD1) HOLD4=0.0
  HCLD4=HOLD4+1.0
  IF(HOLD4.GT.HOLD5) HOLD5=HOLD4
  CONTINUE
KDM=KDM+((HOLD3-HOLD2)/HOLD1)*((HOLD5*12.0*PI)/(180.0*XY))
HCLD6=HCLD6+1.0/XY
CONTINUE
KDM=50.0*KDM/HOLD6
FACT(NFACT)=KDM
END PRATT AND WHITNEY DISTORTION INDEX
PTHCLD(NFACT)=PTAVE
PTIME(NFACT)=NMAP*.125
DEFACT(NFACT)=FACT(NFACT)
START COMPUTATION OF MEAN,STD-DEV,DEFACT(N),TEST FOR STALL WARNING
IF(NFACT.LT.51) GO TO 1076
DEFACT(NFACT)={FACT(NFACT)+FACT(NFACT-1)+FACT(NFACT-2)}/3.0
TE=XMEAN+2.5*STDV
IF(DEFACT(NFACT).LT.TEST) GO TO 1076
WRITE(6,1074) TIME(NFACT)
FORMAT(1,'',** STALL WARNING **',3X,'TIME IS',F8.3/)
CONTINUE
SUM1=SUM1+FACT(NFACT)
IF(JTIME=SUM1) GO TO 1072
XMEAN=SUM1/50.0

```



```

YMEAN(NFACT)=XMEAN
N=NFACT-49
JTIMES=JTIMES+1
SUM2=0.0
DO 1077 I=1,N,NFACT
SUM2=SUM2+(FACT(I)-XMEAN)**2
CONTINUE
1077 STDV=SUM2/49.0
STDV=SQRT(STDV)
YSTDV(NFACT)=STDV
SUM1=0.0
JTIMES=0
CONTINUE
1072 C
END COMPUTATION OF MEAN,STD-DEV,DFACT(N),TEST FOR STALL WARNING
IF(NFACT*GE*NSTOP) GO TO 107
IF(NFACT=NFACT+1
IF (NCASE*GT. 32) GO TO 100
NMAP=NMAP+5
GO TO 700
CONTINUE
107 WRITE(6,1075) STALL OCCURRED AT TIME',F8.2/
FORMAT(6,1006) NRUN,PSSTATC
WRITE(6,1015) ITIMES
WRITE(6,1000)
DO 115 I=1,N,NSTOP
WRITE(6,216)N,DFACT(N),FACT(N),TIME(N),PTHOLD(N),YMEAN(N),YSTDV(N)
CONTINUE
115 C
START PLOT OF DFACT(N) V.S. TIME
DO 1002 N=1,NSTOP
IF(DFACT(N).LT.STALL2(1)) STALL2(1)=DFACT(N)
IF(DFACT(N).GT.STALL2(2)) STALL2(2)=DFACT(N)
CONTINUE
1002 DIFF=STALL2(2)-STALL2(1)
DIFF=DIFF/20.0
DIFF=DIFF
STALL2(1)=STALL2(2)+DIFF
STALL1(1)=STALL2(2)-DIFF
STALL1(2)=STALL2(1)
NSTOP=STALL1(2)
CALL DPAW(N,TIME,DFACT,1,0,TITLE4,TITLE5,0,0,0,0,1,1,8,8,1,L)
CALL DPAW(2,STALL1,STALL2,3,0,TITLE6,TITLE5,0,0,0,0,0,0,8,12,
11,L)
END PLOT OF DFACT(N) V.S. TIME
IF(ITIMES.EQ.64) GO TO 1008
C

```

VANN0258
VANN0259
VANN0260
VANN0331
VANN0332
VANN0333
VANN0334
VANN0335
VANN0336
VANN0337
VANN0338
VANN0339
VANN0340

VANN0261
VANN0262
VANN0263
VANN0264
VANN0265
VANN0266
VANN0267
VANN0268
VANN0269
VANN0270
VANN0271
VANN0272
VANN0273
VANN0274

VANN0275
VANN0276
VANN0277
VANN0278
VANN0279
VANN0280
VANN0281
VANN0282
VANN0283
VANN0284
VANN0285
VANN0286
VANN0287
VANN0288

VANN0289


```
VANN0290
VANN0291
VANN0292
VANN0293
VANN0294
VANN0295
VANN0296
VANN0297
VANN0298
VANN0299
VANN0300
VANN0301
VANN0302
VANN0303
VANN0304
VANN0305
VANN0306
VANN0307
VANN0308
VANN0309
VANN0310
VANN0311
VANN0312
VANN0313
VANN0314
VANN0315
VANN0316
VANN0317
VANN0318
VANN0319
VANN0320
VANN0321
VANN0322
VANN0323
VANN0324
VANN0325
VANN0326
VANN0327
VANN0328
VANN0329
```

```
I STOP=64-ITIMES
DC READ(4,105,END=1024,ERR=1025) TAPED
WRITE(6,1049) I
GC FORMAT(1008)
FCR MAT(17F10.4),160A2)
EFORMAT(4(200A2),**INPUT CHECK***,,/)
2C9 EFORMAT(//,40X,,/)
2C10 EFORMAT(//,15X,5I10)
2C13 ECPHAT(//,15X,**FOR RUN NUMBER',1X,I2,2X,'CASE NUMBER',1X,I4,*
1 ***,//)
216 FCR MAT(.,.,I4,2E15.5,2F12.3,2E15.5)
1C00 FCR MAT(.,.,//3X,N:,7X,DFACT(N)',8X,'TIME',7X,
1 PTAVE,10X,'MEAN',9X,'STD-DEV',//)
1C03 ECR MAT(6A8)
1C06 ECR MAT(.,., CASE NUMBER',I4,/ AVERAGE STATIC PRESSURE IS',
1F12.3//)
1C10 FCR MAT(2I5,2F10.2) WAS READ',I3,' TIMES' /)
1C15 FCR MAT(.,., TAPE WAS READ',I3,
1C149 FCR MAT(.,., TAPE WAS READ',I3,
1 TO TIMES TO POSITION FOR NEXT CASE',/)
1C20 RITE(6,1G22) N
1C22 FCR MAT(.,., END OF TAPE WAS REACHED',/
1 DO 27 N=1,NRUNS',/, WHERE N=',I5)
1C71 ECR MAT(.,., //2X,6A8//)
STOP
1C1021 WRITE(6,1023) N
1C1023 FCR MAT(.,., FORMAT ERROR ON TAPE',/ DO 27 N=1,NRUNS',
1/, WHERE N=',I5)
STOP
1C1024 WRITTE(6,1026) NMAP
1C1026 FCR MAT(.,., END CF TAPE WAS REACHED',/ AFTER 100 CCNTINUE',/
1, WHERE NMAP=',I5)
STOP
1C1025 WPRITE(6,1027) NMAP
1C1027 FCR MAT(.,., FORMAT ERROR ON TAPE',/
1, AFTER 100 CCNTINUE',/ WHERE NMAP=',I5)
STOP
1C1007 STOP
END
FUNCTION UZMACH{PTF,POF}
THIS SUBROUTINE CALCULATES THE AXIAL MACH NUMBER
```

```
G=1.4
A=(G-1.0)/G
B=2.0/(G-1.0)
```


LIST OF REFERENCES

1. Farmer, C. J., Inlet Distortion, Vorticity, and Stall in an Axial Flow Compressor, Master's Thesis, Naval Postgraduate School, Monterey, Calif., 1972.
2. AIAA Paper No. 72-1116, A New Approach To Distortion Induced Compressor Stall--Vorticity Maps, by Lt. Clinton Farmer, Lcdr. Michael Iverson, and Allen Fuhs, 1972.
3. Shoemaker, J. E., An Analysis of the Effects of Instantaneous Vorticity on Compressor Performance, Master's Thesis, Naval Postgraduate School, Monterey, Calif., 1973.
4. Downs, C. P., A Rational Basis for Circumferential Distortion Index Formulation, Master's Thesis, Naval Postgraduate School, Monterey, Calif., to be published 1974.
5. NASA Lewis Research Center Technical Memorandum, Instantaneous Distortion in a Mach 2.5, 40-percent-Internal-Contraction Inlet and its Effect on Turbojet Stall Margin, by Paul L. Burstadt and James E. Calogeras, to be published 1974.
6. AIAA Paper No. 71-667, Instantaneous and Dynamic Analysis of Supersonic Inlet-Engine Compatibility, by J. E. Calogeras, P. L. Burstadt, and R. E. Coltrin, 1971.
7. AIAA Paper No. 73-1316, The Effect of Inlet Temperature and Pressure Distortion on Turbojet Performance, by W. M. Braithwaite, E. J. Graber, Jr., and C. M. Mehalic, 1973.
8. AGARD NATO Lecture Series No. 53, Ref 6, Dynamic Characteristics of Engine Inlets, by D. Zonars, 1972.
9. NASA Edwards Technical Note No. D-7328, Steady-State and Dynamic Pressure Phenomena in the Propulsion System of an F-111A Airplane, by F. W. Burcham, Jr., D. L. Hughes, and J. K. Holzman, 1973.

INITIAL DISTRIBUTION LIST

	No. Copies
1. Defense Documentation Center Cameron Station Alexandria, Virginia 22314	2
2. Library, Code 0212 Naval Postgraduate School Monterey, California 93940	2
3. Chairman, Department of Aeronautics, Code 57Be Naval Postgraduate School Monterey, California 93940	1
4. LTjg James E. Shoemaker 113 Norton Street Bennington, Vermont 05201	1
5. Professor Allen E. Fuhs, Code 57 Fu Department of Aeronautics Naval Postgraduate School Monterey, California 93940	10
6. LT John L. Vann 1840 Lynnhaven Rd. Ft. Worth, Texas 76103	3
7. Professor M. F. Platzer, Code 57Pl Department of Aeronautics Naval Postgraduate School Monterey, California 93940	1
8. Mr. Joe Boytos Naval Air Propulsion Test Center Trenton, New Jersey 08628	1
9. Dr. Herbert Mueller, Code 310A Naval Air Systems Command Washington, D. C. 20360	1
10. Dr. Frank Tanczos, Code 03 Naval Air Systems Command Washington, D. C. 20360	1
11. Mr. Karl Guttman, Code 330 Naval Air Systems Command Washington, D. C. 20360	1

12. Dr. H. O. Johnson, Code 330 1
Naval Air Systems Command
Washington, D. C. 20360
13. Mr. Robert Brown, Code 536 1
Naval Air Systems Command
Washington, D. C. 20360
14. Dr. Ralph Roberts 1
Office of Naval Research
800 North Quincy Street
Arlington, Virginia 22217
15. Mr. Eric Lister 1
R. & T. Division
Naval Air Propulsion Test Center
Trenton, New Jersey 08628
16. Mr. Albert Martino 1
R. & T. Division
Naval Air Propulsion Test Center
Trenton, New Jersey 08628
17. Mr. James Patton, Jr. 1
Office of Naval Research
Arlington, Virginia 22218
18. Mr. Ivan Bush 1
AFAPL
WPAFB, Ohio 45433
19. M. l'Ingenieur en Chef Marc Pianko 1
Service Technique Aeronautique
4 Avenue de la Porte d'Issy
75 Paris 15eme FRANCE
20. Mr. J. Surugue 1
Directeur, Energie et Propulsion
ONERA
29 Avenue de la Division Leclerc
92 Chatillon-sous-Bagneux, FRANCE
21. Dr. John Dunham 1
National Gas Turbine Establishment
Pyestock
Farnborough Hants GREAT BRITAIN
22. Professor Kuhl 1
D. V. L.
505 Porz Wahn
Linder Hohe
Allemagne GERMANY

23. Mr. Clifford Simpson 1
AFAPL/TB
Wright-Patterson A.F.B., Ohio 45433
24. Professor Gordon Oates 1
University of Washington
Seattle, Washington 98105
25. Professor Robert Goulard 1
Director, Project SQUID
Purdue University
Lafayette, Indiana 47907
26. Mr. J. F. Chevalier 1
SNECMA
Centre d'Essais de Villaroche
77 Moissy-Cramayel FRANCE
27. Mr. M. Van Staveren 1
Institute for Applied Research TNO
Post bus 406
Delft NETHERLANDS
28. Mr. Hill Barrett 1
Detroit Diesel Allison
General Motors Corp.
Indianapolis, Indiana 46206
29. Professor Antonio Ferri 1
Department of Aeronautics and Astronautics
School of Engineering and Science
New York University
Bronx, New York 10453
30. Mr. Elmer G. Johnson 1
Director, Fluid Dynamics Facilities Research
Laboratory
USAF Aerospace Research Laboratories
Wright-Patterson A.F.B., Ohio 45433
31. Dr. A. A. Mikolajczak 1
Pratt and Whitney Aircraft
East Hartford, Conn. 06108
32. Dr. Peter Tramm 1
Detroit Diesel Allison
General Motors Corp.
Indianapolis, Indiana 46206
33. Professor Duncan Rannie 1
California Institute of Technology
Pasadena, California 91109

34. Professor Jack Kerrebrock 1
Aeronautics and Astronautics
Massachusetts Institute of Technology
Cambridge, Massachusetts 02138
35. Professor George Serovy 1
Iowa State University
Ames, Iowa 50010
36. Dr. Gary R. Ludwig 1
Aerodynamics Research
Cornell Aeronautical Laboratory, Inc.
Buffalo, New York 14221
37. Mr. James E. Calogeras 1
NASA Lewis Research Center
Cleveland, Ohio 44135
38. Dr. Gunnar Broman 1
Vice President, Engineering
VOLVO Flygmotor
Trollhattan, SWEDEN
39. Mr. Robert Zalis 1
MZ 240 GF
1000 Western Avenue
Lynn, Massachusetts 01910
40. Mr. Paul H. Kutschenreuter, Jr. 1
Mail Drop E 198
General Electric Company
Cincinnati, Ohio 45215
41. Mr. David Jamison 1
General Electric Company
P.O. Box 2143
Kettering Branch
Dayton, Ohio 45429
42. Prof. Jacques Valensi 1
Director Institut de Mecanique des Fluides
l 'Universite d'Aix-Marseille
Marseille, FRANCE
43. Professor Jacques Chauvin 1
Von Karman Institute for Fluid Mechanics
72 Chaussee de Waterloo
1640 Rhode-St-Genese BELGIUM
44. Mr. Marvin F. Schmidt 1
Turbine Engine Division
AFAPL
Wright-Patterson A.F.B., Ohio 45433

45. Mr. J. W. McBride 1
General Electric Company
Evandale, Ohio 45215
46. Dr. Leroy H. Smith, Jr. 1
General Electric Company
Evandale, Ohio 45215
47. Professor B. Lakshminarayana 1
MIT Gas Turbine Laboratory
Massachusetts Institute of Technology
Cambridge, Massachusetts 02138
48. Professor Jean Louis 1
MIT Gas Turbine Laboratory
Massachusetts Institute of Technology
Cambridge, Massachusetts 02138
49. Dr. F. O. Carta 1
United Aircraft Research Labs.
United Aircraft Corporation
400 Main Street
East Hartford, Connecticut 06108
50. Mr. Norman Cotter 1
Pratt and Whitney Florida Research Center
West Palm Beach, Florida 33402
51. Dr. George L. Mellor 1
Princeton University
Forrestal Campus
Princeton, New Jersey 08540
52. Mr. Stan Ellis 1
Pratt and Whitney Florida Research Center
West Palm Beach, Florida 33402
53. Mr. David Bowditch 1
HASA Lewis Research Center
Cleveland, Ohio 44135
54. Professor Frank Marble 1
California Institute of Technology
Pasadena, California 91109
55. Professor Bruce A. Reese 1
School of Mechanical Engineering
Purdue University
Lafayette, Indiana 47907

56. Professor T. C. Adamson, Jr. 1
Dept. of Aerospace Engineering
University of Michigan
Ann Arbor, Michigan 48103
57. Professor W. R. Sears 1
University of Arizona
Tucson, Arizona 85721
58. Professor J. E. McCune 1
M.I.T. - 37 - 391
Cambridge, Massachusetts 02139
59. Dr. Jack Nielsen 1
Nielsen Engineering and Research, Inc.
850 Maude Avenue
Mountain View, California 94040
60. W. F. O'Brien 1
Mechanical Engineering Dept.
Virginia Polytechnic Institute and State
University
Blacksburg, Virginia 24061
61. Dr. W. Heiser 1
AFAPL
Wright-Patterson A.F.B., Ohio 45433
62. CAPT Barry Brownstein 1
Air Force Aero-Propulsion Laboratory
Wright-Patterson A.F.B., Ohio 45433
63. Mr. Paul L. Burstadt 1
Lewis Research Center
National Aeronautics and Space Administration
Cleveland, Ohio 44135
64. Lcdr. C. Downs 1
6200 N.W. 8th Street
Oklahoma City, Oklahoma 73127



Thesis
V184
c.1

Vann

153708

Formulation and comparison of instantaneous distortion indices for assessing compressor stall.

Thesis
V184
c.1

Vann

153708

Formulation and comparison of instantaneous distortion indices for assessing compressor stall.

thesV184

Formulation and comparison of instantane



3 2768 002 05379 5

DUDLEY KNOX LIBRARY